Fig. 1 (a,b) Skull X-ray shows a catheter inserted in the lateral ventricle. (c) Abdominal X-ray shows implanted pump on the abdominal wall and a catheter connected from the pump under the skin.

University. Written informed consent was obtained from the patients and/or family members after detailed explanation of the procedures was provided. Intraventricular PPS infusion was carried out in 11 patients with prion diseases, including four men and seven women with mean age of 64.9 years (range, 39–73) at Fukuoka University from 2004. Eligible patients had probable prion diseases according to WHO criteria,[13] normal hematology, and normal renal and hepatic function. Patients undergoing continuous treatment with anticoagulants such as warfarin, heparin, clopidogrel, or aspirin and those presenting with clinical symptoms caused by increased intracranial pressure and/or edema of the brain, active viral, bacterial, or fungal infection causative of either oral temperature > 38°C or clinically significant leukocytosis, and viral syndromes clinically diagnosed within 2 weeks prior to start of test therapy, were excluded.

Treatment

The patients had a single standard ventricular catheter placed in the anterior horn of the right lateral ventricle, unless clinical reasons dictated another point of access to the ventricular system. The catheter was connected to a subcutaneous infusion pump (Archimedes, 20 mL reservoir, flow rate 0.5 mL/24 h; Codman Inc., Raynham, MA

US) implanted subcutaneously in the right upper abdominal wall (Fig. 1). Seven days after the surgical procedure, brain CT scan was performed (Fig. 2) to confirm no surgical complications. Then, PPS infusion was started via the implanted pump. PPS (pentosan polysulphate SP 54) was obtained from beneArzneimittel GmbH (Munich, Germany). Intraventricular PPS infusion started at a dosage of 1 μg/kg/day then was gradually escalated to the target dosage of 120 μg/kg/day; the dosage proceeded to the next higher level after the absence of adverse effects was confirmed. Pump refilling with PPS was performed every 4 weeks. Patients' conditions were checked thoroughly on a weekly basis in the first 4 weeks after commencement of PPS infusion, and on a monthly basis thereafter.

Assessment

This was an open prospective study in newly diagnosed patients with prion diseases. The primary endpoint was overall survival; secondary endpoints were 6-month survival, neurological status, and activities of daily living (ADL) assessed at 6, 12, and 18 months after start of treatment. The patients were considered to be part of the study from the commencement of PPS administration until discontinuation of PPS because of adverse effects, death, or start of another treatment.
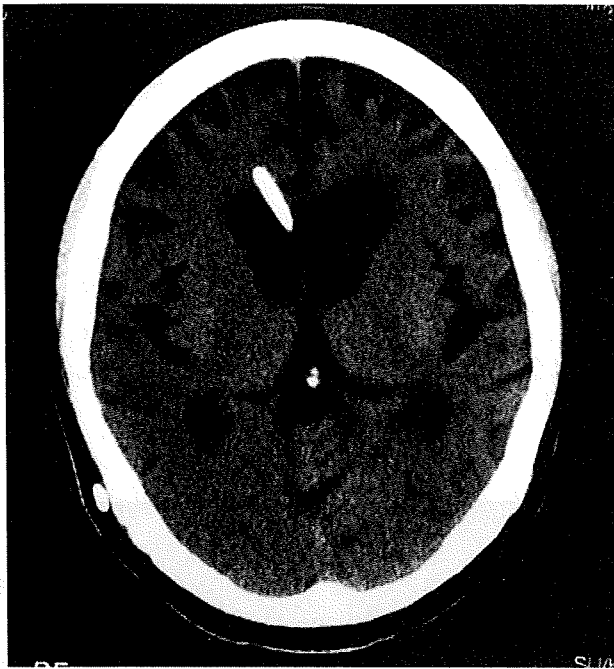
Fig. 2 CT scan 1 week after implantation shows that there are no complications such as bleeding.

Follow-up examinations included physical and neurological examinations, laboratory tests, electroencephalography, and head CT scans every 4 weeks. If applicable, head MRI scans with contrast were performed every 8 weeks. Evaluation of ADL including modified Rankin scaling was conducted every 6 months.

Adverse events

Adverse events related to PPS treatment were defined as all clinical abnormalities that appeared in patients during the study period. Abnormal laboratory results during the study period were considered as adverse events when the immediate relationship could be demonstrated.

RESULTS AND DISCUSSION

Eleven patients were enrolled in total: three cases of genetic prion diseases (familial CJD with V180I mutation, $n = 2$; GSS with P102L mutation, $n = 1$); two iatrogenic CJD; and six sporadic CJD (Table 1). Two cases with iatrogenic CJD were due to cadaver dura mater graft 18 and 24 years before the onset of the illness, respectively. Seven patients died, all due to sepsis or pneumonia. The four remaining patients continue to receive treatment with PPS 120 μg/kg/day infusions. These include sporadic CJD in two cases, including one MM2 cortical form diagnosed with biopsied specimen; and I180V mutation in the *PRNP* gene

confirmed in another two cases. All the four cases have shown longer survival periods compared with previously reported cases. At the most recent estimate, mean survival after commencement of intraventricular PPS infusion was 24.2 months (range, 4–49). Mean modified Rankin score at start of treatment was 3.5 (range, 2–5); as of very recently this rose to 5.2 (range, 4–6). All cases treated with intraventricular PPS infusion have shown deterioration of brain function of various degrees. Subdural fluid collection was observed on CT scans in most (10 of 11) cases (Fig. 3). Phenitoin-controllable epileptic jerks were observed in one case. Except for these, no other adverse effects were observed during the treatment. No abnormalities in blood cell counts, serum chemistry, and coagulation tests were recognized.

To date in our clinical trial, PPS at a dosage of 120 μg/kg/day was well tolerated with no serious adverse effects observed. In most patients intraventricular PPS was associated with subdural fluid collection to various degrees, although this adverse effect did not influence their clinical conditions. Although thrombocytopenia and coagulation abnormality are known to occur occasionally with PPS,[14] such adverse effects were not observed in our patients.

Pentosan polysulfate, a large polyglycoside molecule with weak heparin-like activity, has been shown to prolong significantly the incubation period of PrP^{Sc} in a rodent scrapie model.[12] Clinically, the first treatment using intraventricular PPS was performed in a young man with vCJD.[15] At age 16 years, he developed behavioral disturbance followed by progressive ataxia, pyramidal signs and myoclonus, which led to the diagnosis of possible vCJD. At the time of first administration of PPS, the patient already had symptoms of advanced vCJD including ataxia, cognitive decline, dysphagia, and myoclonus, and was bedridden. A catheter was implanted in the anterior horn of the right lateral ventricle and connected to a programable pump implanted subcutaneously in the abdomen. Intraventricular administration of PPS did not elicit any systemic adverse effect. Follow-up CT scans demonstrated subdural fluid collections first over the right hemisphere and subsequently over the left hemisphere, necessitating surgical intervention.

This first patient is currently still alive and in stable neurological condition. PPS has been administered intraventricularly to the patient for 6 years. Although there were no major improvements in his neurological and general condition, there were a few notable changes in the brainstem function.

Since January 2003, more than 25 patients with different prion diseases have been treated with continuous intraventricular administration of PPS.[16–19] Although most reports have concluded that the treatment does not cause severe adverse effects, regrettably there are also no clear benefits

Table 1 Summary of clinical data of all 11 patients with intraventricular pentosan polysulfate (PPS) administration

No.	Age at surgery	Gender	Diagnosis	Date of surgery	PPS dose initial/final (μg/kg/day)	Duration from the onset (months)	Survival from the surgery (months)
1	67	F	sCJD	2004/11/16	1/120	9	17†
2	73	F	sCJD	2005/3/1	2/120	3	20†
3	68	F	sCJD (MM2)	2005/6/2	10/120	6	49
4	64	F	fCJD (V180I)	2005/6/21	10/120	4	49
5	64	F	sCJD	2005/11/14	10/120	3	25†
6	55	M	iCJD	2006/3/13	10/120	10	4†
7	66	M	iCJD	2006/6/12	20/120	3	9†
8	69	F	GSS (P102L)	2006/8/2	20/120	6	14†
9	73	F	fCJD (V180I)	2006/10/15	20/120	7	34
10	68	M	sCJD	2007/3/7	20/120	4	18†
11	39	F	sCJD	2007/4/3	20/120	20	27

†Patient deceased. sCJD, sporadic CJD; fCJD, familial CJD; iCJD, iatrogenic CJD
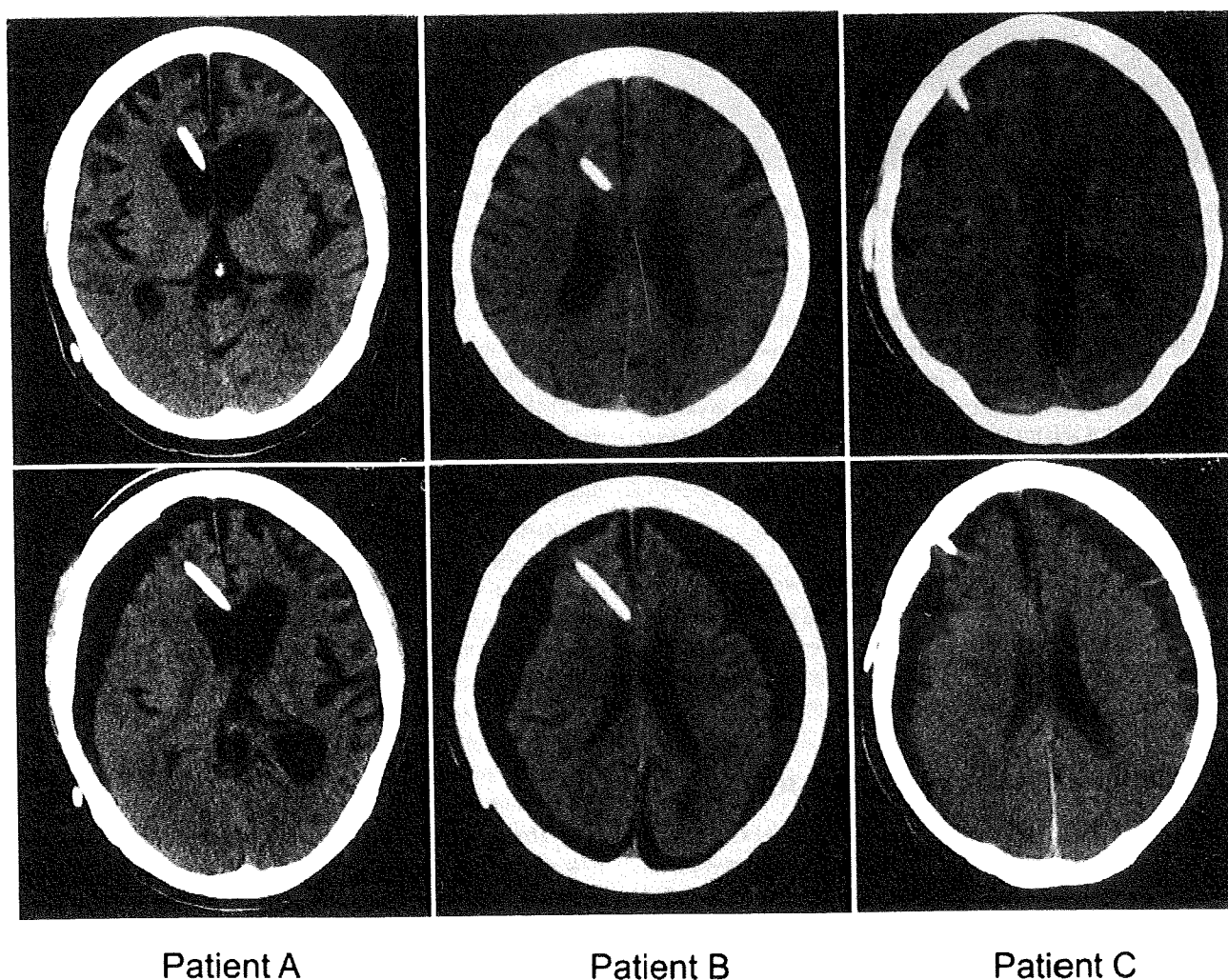

Patient A   Patient B   Patient C

Fig. 3 Non-enhanced serial CT scans of three patients with treatment of pentosan polysulfate (PPS) administration. Upper panels show CT scans at start of PPS administration. Lower panels show CT scan of each patient at 4 months (patient A), 5 months (patient B), and 8 months (patient C) after the start of PPS administration. Note that subdural fluid collections over one or both hemispheres are observed on all lower panel CT scans.

© 2009 Japanese Society of Neuropathology

against disease progression. PPS is neither able to reverse the clinical course of advanced disease, nor able to achieve functional recovery of established neurological deficits. Moreover, it remains unclear whether higher doses of the drug may exert better outcomes. Further experimental animal studies should be done to investigate optimal PPS dose and its effects on survival and to show the extent to which the drug penetrates and spreads throughout the brain.

Post mortem examination might support the efficacy of PPS for reducing abnormal prion deposit in the brain. In one sporadic CJD case treated with intraventricular PPS in the present study, quantitative Western blot analysis revealed that the level of abnormal protease-resistant PrP was reduced considerably compared with in individuals who had never been treated with intraventricular PPS (data not shown). Further formal, prospective, longitudinal, standardized studies, including post mortem investigation, are recommended.

ACKNOWLEDGEMENTS

REFERENCES

1. Prusiner SB. Prions. *Proc Natl Acad Sci USA* 1998; **95**: 13363–13383.
2. Will RG, Ironside JW, Zeidler M *et al.* A new variant of Creutzfeldt-Jakob disease in the UK. *Lancet* 1996; **347**: 921–925.
3. Brown P, Preece M, Brandel JP *et al.* Iatrogenic Creutzfeldt-Jakob disease at the millennium. *Neurology* 2000; **55**: 1075–1081.
4. Caughey B, Raymond GJ. Sulfated polyanion inhibition of scrapie-associated PrP accumulation in cultured cells. *J Virol* 1993; **67**: 643–650.
5. Kimberlin RH, Walker CA. The antiviral compound HPA-23 can prevent scrapie when administered at the time of infection. *Arch Virol* 1983; **78**: 9–18.
6. Ehlers B, Diringer H. Dextran sulphate 500 delays and prevents mouse scrapie by impairment of agent replication in spleen. *J Gen Virol* 1984; **65**: 1325–1330.
7. Farquhar CF, Dickinson AG. Prolongation of scrapie incubation period by an injection of dextran sulphate 500 within the month before or after infection. *J Gen Virol* 1986; **67**: 463–473.
8. Kimberlin RH, Walker CA. Suppression of scrapie infection in mice by heteropolyanion 23, dextran sulfate, and some other polyanions. *Antimicrob Agents Chemother* 1986; **30**: 409–413.
9. Diringer H, Ehlers B. Chemoprophylaxis of scrapie in mice. *J Gen Virol* 1991; **72**: 457–460.
10. Ladogana A, Casaccia P, Ingrosso L *et al.* Sulphate polyanions prolong the incubation period of scrapie-infected hamsters. *J Gen Virol* 1992; **73**: 661–665.
11. Farquhar C, Dickinson A, Bruce M. Prophylactic potential of pentosan polysulphate in transmissible spongiform encephalopathies. *Lancet* 1999; **353**: 117.
12. Doh-ura K, Ishikawa K, Murakami-Kubo I *et al.* Treatment of transmissible spongiform encephalopathy by intraventricular drug infusion in animal models. *J Virol* 2004; **78**: 4999–5006.
13. Zeidler M, Gibbs CJ Jr, Meslin F. *WHO Manual for Strengthening Diagnosis and Surveillance of Creutzfeldt–Jakob Disease.* Geneva: World Health Organization, 1998; 47–51.
14. Tardy-Poncet B, Tardy B, Grelac F *et al.* Pentosan polysulfate-induced thrombocytopenia and thrombosis. *Am J Hematol* 1994; **45**: 252–257.
15. Parry A, Baker I, Stacey R, Wimalaratna S. Long term survival in a patient with variant Creutzfeldt-Jakob disease treated with intraventricular pentosan polysulphate. *J Neurol Neurosurg Psychiatry* 2007; **78**: 733–734.
16. Todd NV, Morrow J, Doh-ura K *et al.* Cerebroventricular infusion of pentosan polysulphate in human variant Creutzfeldt–Jakob disease. *J Infect* 2005; **50**: 394–396.
17. Whittle IR, Knight RSG, Will RG. Unsuccessful intraventricular pentosan polysulphate treatment of variant Creutzfeldt-Jakob disease. *Acta Neurochir (Wien)* 2006; **148**: 677–679.
18. Rainov NG, Tsuboi Y, Krolak-Salmon P *et al.* Experimental treatments for human transmissible spongiform encephalopathies: is there a role for pentosan polysulfate? *Expert Opin Biol Ther* 2007; **7**: 713–726.
19. Bone I, Belton L, Walker AS, Darbyshire J. Intraventricular pentosan polysulphate in human prion diseases: an observational study in the UK. *Eur J Neurol* 2008; **15**: 458–464.

RESEARCH ARTICLE

Autoantibody to glial fibrillary acidic protein in the sera of cattle with bovine spongiform encephalopathy

Sachiko Nomura[1], Taku Miyasho[1], Naoyuki Maeda[2], Katsumi Doh-ura[3] and Hiroshi Yokota[1]

[1] Department of Veterinary Biochemistry, Rakuno Gakuen University, Ebetsu, Hokkaido, Japan
[2] Department of Technology, Association of Meat Science and Technology Institute, Tokyo Japan
[3] Department of Prion Research, Tohoku University Graduate School of Medicine, Sendai, Japan

It is desirable to make the diagnosis in live cattle with bovine spongiform encephalopathy (BSE), and thus surrogate markers for the disease have been eagerly sought. Serum proteins from BSE cattle were analyzed by 2-D Western blotting and TOF-MS. Autoantibodies against proteins in cytoskeletal fractions prepared from normal bovine brains were found in the sera of BSE cattle. The protein recognized was identified to be glial fibrillary acidic protein (GFAP), which is expressed mainly in astrocytes in the brain. The antigen protein, GFAP, was also found in the sera of BSE cattle. The percentages of both positive sera in the autoantibody and GFAP were 44.0% for the BSE cattle, 0% for the healthy cattle, and 5.0% for the clinically suspected BSE-negative cattle. A significant relationship between the presence of GFAP and the expression of its autoantibody in the serum was recognized in the BSE cattle. These findings suggest a leakage of GFAP into the peripheral blood during neurodegeneration associated with BSE, accompanied by the autoantibody production, and might be useful in understanding the pathogenesis and in developing a serological diagnosis of BSE in live cattle.

1   Introduction

Prion diseases, or transmissible spongiform encephalopathies (TSEs), are characterized by progressive neurodegeneration associated with the accumulation of the abnormal isoform of the prion protein in neuronal tissues in humans and animals. This abnormal isoform of the prion protein is suggested to be a main component of the pathological agent, the prion [1]. Astrocytosis, neuronal cell loss, and abnormal prion protein deposition are the hallmarks of the neuropathology of TSEs [2], and the mechanisms of both

prion-induced neurodegeneration and prion replication are still controversial. Among the TSEs, bovine spongiform encephalopathy (BSE) has had a wide influence on the economics of cattle production. Since 1972, more than 180 000 cattle have been infected with BSE. The disease has been assumed to be a cause of variant Creutzfeldt–Jakob disease (vCJD), which has been reported in young people in the United Kingdom and other countries [3].

Currently, a BSE diagnosis is made by detecting abnormal prion protein in the brain post-mortem. However, it is desirable to make the diagnosis in live cattle, and thus surrogate markers for the disease have been eagerly sought. This is also the case with human TSEs because of increasing concerns about safety issues regarding human blood and blood products, especially in the United Kingdom and other countries affected by BSE. Among the candidates previously considered, brain components and/or autoantibodies against them in the peripheral blood remain interesting. Toh *et al.* [4, 5] reported that autoantibodies against neurofilament proteins (of 200, 150 and

Correspondence: Professor Hiroshi Yokota, Department of Veterinary Biochemistry, School of Veterinary Medicine, Rakuno Gakuen University, Ebetsu, Hokkaido 069-8501, Japan
E-mail: h-yokota@rakuno.ac.jp
Fax: +81-11-388-4743

Abbreviations: BSE, bovine spongiform encephalopathy; **CJD,** Creutzfeldt–Jakob disease; **GFAP,** glial fibrillary acidic protein; **TSEs,** transmissible spongiform encephalopathies

InterScience®   **www.proteomics-journal.com**

70 kDa) were detected in approximately 55–78% of serum samples obtained from human patients with kuru (an acquired type of human TSE), CJD and other neurological diseases. However, the antibodies were also detected in 28–67% of healthy subjects. Tiwana *et al.* [6] reported detection of polyclonal antibodies against *Acinetobacter*, which has amino acid sequences similar to those of neurofilament proteins. Wilson *et al.* [7] assumed that the immunocompetence of BSE cattle was reduced such that such cattle were readily infected with various bacteria, and some of the antibodies produced were reactive against neurofilament protein antigens.

We report in this study that both glial fibrillary acidic protein (GFAP) and its autoantibody in the serum were recognized in a significantly increased number of BSE cattle compared with healthy cattle or BSE-suspected cattle that tested negative.

2   Materials and methods

2.1   Materials

Serum samples from BSE cattle and clinically suspected cattle with negative BSE tests were obtained from the Veterinary Laboratories Agency, Weybridge, UK. Individuals infected with BSE were diagnosed by immunohistochemistry and immunoblotting for abnormal prion protein in the brain. The cattle with negative BSE tests that had been suspected to have BSE clinically were negative for any abnormal prion protein accumulation in the brain. The sera were also obtained from healthy cattle raised in Japan. A polyclonal antibody against human GFAP was purchased from MP Biochemicals, Ohio, USA, and bovine GFAP was obtained from PROGEN Biotechnik GmbH, Gaithersburg, MD, USA.

2.2   Preparation of subcellular fractions

The subcellular fractions were prepared using a ProteoExtract™ Subcellular Proteome Extraction Kit (Merck, NJ, USA) as described in the manufacturer's instructions.

2.3   SDS-PAGE and immunoblotting

Equal amounts of protein were resolved by SDS-PAGE according to the method of Laemmli [8]. For analysis, protein was electroblotted from the polyacrylamide gel onto a PVDF membrane using the method of Towbin *et al.* [9]. Immunoblotting analysis was performed using serum samples from cattle with BSE as the primary antibody (diluted at 1:1000) and HRP-conjugated anti-bovine IgG as the secondary antibody (diluted at 1:2000). Immu-

noreactive bands on the membrane were detected using ECL™ Western blotting detection reagents (Amersham Bioscience).

2.4   2-D immunoblotting

IEF was conducted using 11 cm IPG strips with a linear pH gradient of 3–10 (GE Healthcare). Solubilized samples were combined with rehydration buffer [8 M urea, 4% CHAPS, 18 mM DTT, 0.5% IPG buffer, trace amount of bromophenol blue (BPB)] to a final volume of 250 μL. The resulting sample preparations were loaded into the IPG strip holder, and swelling of the IPG strips proceeded for 14 h at room temperature. IEF was run following a step-wise voltage increase procedure: 300 V for 1 min, 3500 V for 4 h. After IEF, the strip was subjected to two-step equilibration in equilibration buffer containing 6 M urea, 30% glycerol, 2% SDS and 50 mM Tris-HCl (pH 8.8) with 65 mM DTT, w/v, for the first step, and the same buffer containing 135 mM iodoacetamide instead of DTT for the second step. The strip was then transferred onto the 2-D SDS-PAGE gel made of 1.5-mm-thick 10% polyacrylamide. Electrophoresis was performed for 30 min, and after the removal of the IPTG strip, it was performed for 1.5 h at 20 mA. The resultant gel was stained with CBB R-250. Immunoblotting analysis was performed using the sera from cattle with BSE as a primary antibody and HRP-conjugated anti-bovine IgG as the secondary antibody. Immunoreactive spots were detected using ECL™ Western blotting detection reagents. Estimation of GFAP content ("–" and "+") was determined by using 60 μg of serum protein. The signal levels of "+" approximately corresponded to more than 50 ng GFAP (13 μg/mL in the serum), which were determined by densitometry of the immunoblotting spots using the bovine GFAP standard.

2.5   In-gel digestion for MS analysis

After 2-D electrophoresis and immunoblotting, the targeted protein spot was clipped out of the gel. The clipped gel was incubated in a tube with 100 μL of 50 mM NH₄HCO₃ in 50% methanol solution at room temperature for 10 min for destaining. The destaining step was repeated twice. After removal of the solution, the gel was washed by shaking in 100 μL of 25 mM NH₄HCO₃ solution and was shrunk using 100 μL ACN. After the removal of ACN by centrifugation, the gel pieces were suspended in 10 μL digestion solution (10 μg/mL trypsin in 25 mM NH₄HCO₃). Following this, 10 μL of 100 mM Tris-HCl buffer (pH 8.8) was added and the reaction medium was incubated overnight at 37°C. TFA solution (5%, 50 μL) containing 50% ACN was added to the gel and the tube was shaken at room temperature for 10 min. After centrifugation, the supernatant solution was collected. These extraction processes were repeated twice.

The trypsin-digested solution was concentrated to 20 µL using the speed vac evaporator.

2.6 PMF

The trypsin-digested solution was treated in a ZipTip™ (Millipore) column for removal of contaminant salts. The ZipTip™ column was wetted with 50% ACN in 0.1% TFA. The digested fragments were absorbed onto the column and then the column was washed with 0.1% TFA for removal of salts. The peptide fragments were eluted using 2 µL of 50% ACN in 0.1% TFA with matrix (α-CHCA). The eluted peptide solution was dried on the target plate of a mass analyzer. MS was performed using a instrument (Bruker, autoflex) in the reflect mode with a nitrogen laser (337 nm). The protein was identified using the Mascot search program on the NCBI nr database.

2.7 Dot-blot analysis

Purified bovine GFAP was dissolved in PBS and dotted to a nitrocellulose sheet. Immunobinding analysis was performed using the sera from cattle with BSE as a primary antibody and HRP-conjugated anti-bovine IgG as the secondary antibody. Immunoreactive spots were detected using ECL™ Western blotting detection reagents. Estimation of the autoantibody content ("−" and "+") was determined by using the serum 200-fold diluted with PBS. The signal levels of "−" and "+" corresponded to the antibody titers incapable and capable of detecting 0.1 µg of the bovine GFAP standard, respectively.

2.8 Statistical analysis

Statistical analyses were performed using a nonparametric χ^2 test (Yates' continuity correction) or Fisher's exact method. All tests were two-tailed.

3 Results

3.1 Autoantibodies

Immunoblotting analysis of proteins from various normal bovine tissues was performed using sera from cattle with BSE as a primary antibody to detect autoantibodies expressed in the serum of cattle with the disease. Bands positive on immunoblotting analysis were observed in the brain homogenate (data not shown). Brain homogenates of normal mice and cattle were further separated to give several subcellular fractions. The proteins in each subcellular fraction were analyzed by immunoblotting using BSE sera, and the results are shown in Fig. 1A and B. A band that was positive on immunoblotting analysis with a molecular weight of 50–53 kDa was found in the cytoskeletal fraction prepared from the brains of both species (Fig. 1A and B, lane 4) by using the serum from a BSE cow. On the contrary, no protein band was observed by using the serum from a clinically suspected cow with negative BSE tests (Fig. 1A and B, lanes 5–8). For further investigation of the antigen, cytoskeletal proteins prepared from mouse cerebellum were further purified by 2-D SDS-PAGE and the positive spot was visualized by immunoblotting analysis using the serum from a BSE cow. The CBB-stained gel data and the immunoblotting data are shown in Fig. 2A and B, respectively. An immunopositive spot (Fig. 2B) and the corresponding protein spot
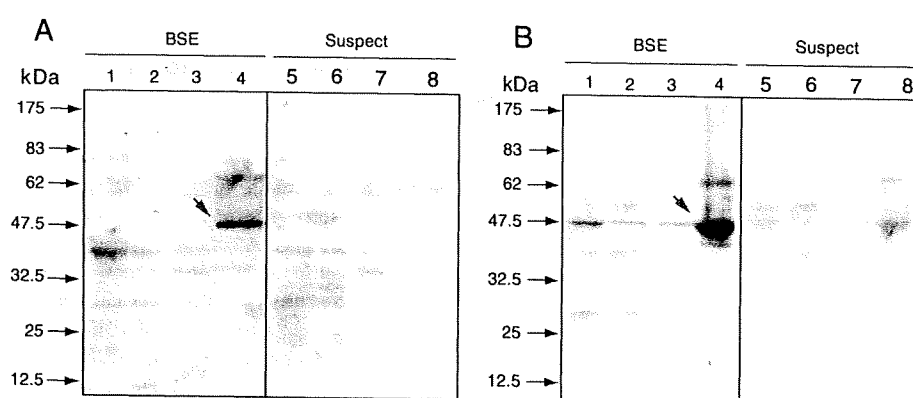

Figure 1. Autoantibody detection in the serum from a cow with BSE. Cerebellar proteins from normal mice (A) and cattle (B) were fractionated into four subcellular fractions (lane 1: cytoplasm; lane 2: cell membrane and organelles; lane 3: nucleus; lane 4: cytoskeletal proteins). Fractionated proteins were subjected to SDS-PAGE and immunoblotting analysis using the serum from a BSE cow (cow no. 2 in Fig. 4B) (BSE; lanes 1–4) or a BSE-suspected test-negative cow (cow no. 2 in Fig. 4B) (suspect; lanes 5–8) as a primary antibody, as described in Section 2. Arrows indicate immunoreactive 50–55 kDa proteins expressed in the cerebellum.
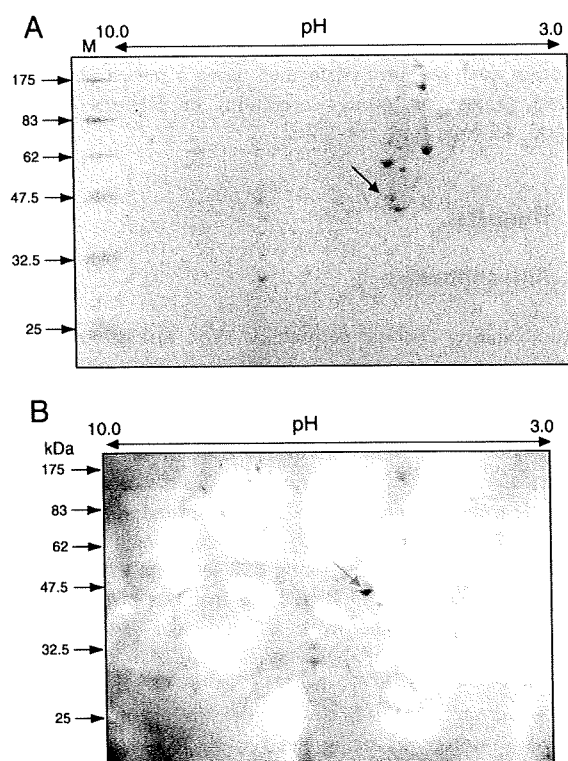
A

B

Figure 2. 2-D electrophoresis and immunoblotting analysis of cytoskeletal proteins. A normal mouse cerebellum was homogenized and fractionated. The cytoskeleton proteins (50 μg) were separated by 2-D SDS-PAGE (CBB-stain) (A). The separated proteins were electroblotted on to a nylon membrane. Immunoreaction was performed using the serum from a BSE cow (cow no. 2 in Fig. 4B) as a primary antibody, as described in Section 2. An arrow in (A) indicates a cluster of positive spots on immunoblotting analysis pointed to by an arrow in (B). Protein markers are shown in the M lane.

```
MERRRITSAR RSYASETVVR GLGPSRQLGT MPRFSLSRMT PPLPARVDFS  50
LAGALNAGFK ETRASERAEM MELNDRFASY IEKVRFLEQQ NKALAAELNQ 100
LRAKEPTKLA DVYQAELREL RLRLDQLTAN SARLEVERDN FAQDLGTLRQ 150
KLQDETNLRL EAENNLAAYR QEADEATLAR VDLERKVESL EEEIQFLRKI 200
YEEVRELRE QLAQQQVHVE MDVAKPDLTA ALREIRTQYE AVATSNMQET 250
EEWYRSKFAD LTDAASRNAE LLRQAKHEAN DYRRQLQALT CDLESLRGTN 300
ESLERQMREQ EERHARESAS YQEALARLEE EGQSLKEEMA RHLQEYQDLL 350
NVKLALDIEI ATYRKLLEGE ENRITIPVQT FSNLQIRETS LDTKSVSEGH 400
LKRNIVVKTV EMRDGEVIKD SKQEHKDVVM 430
```

Figure 3. Identification of the protein antigen by PMF. CBB-stained 2-D PAGE gel area corresponding to the spot immunoreactive to the serum of a BSE cow was cut and digested in the gel with trypsin. The PMF data were obtained by MALDI-TOF-MS analysis as described in Section 2. Several matched proteins were indicated by the MASCOT database search. Six of the best-matched candidate proteins were shown to be GFAP. The sequences found in the PMF are shown with underlining.

(Fig. 2A) were observed. The protein spot was localized in the gel area with an isoelectric point of about pH 5.0–5.5 and a molecular weight of approximately 50–53 kDa.

3.2 Identification of antigen

For identification of the antigen protein, the gel containing the positive spot was prepared and the protein in the spot was digested with trypsin. The digested fragments were analyzed by MALDI-TOF-MS as described in Section 2. The mass data were analyzed by MASCOT using the NCBI database. Six candidate proteins with a high possibility (greater than 75) of matching scores (significant at $p<0.05$) were listed, and the six candidates were identified as a single protein: GFAP (Fig. 3). The MS data obtained from the fragments were matched with the complete amino acid sequence of GFAP. These data indicate that the antigen protein is the cytoskeletal protein GFAP having a 52 kDa molecular weight [10].

3.3 Detection of serum GFAP

To investigate whether the antigen GFAP is present in the serum of the autoantibody-positive BSE cow, serum proteins from the cow were analyzed by 2-D SDS-PAGE and immunoblotting using an antibody against the C-terminus of human GFAP, which is a conserved sequence in the protein sequences of several animals, including humans, rats, mice, and cattle. Purified bovine GFAP as a control showed several spots on the 2-D PAGE (Fig. 4A) and in immunoblotting by using the anti-GFAP antibody (Fig. 4B). No positive spots were observed in the serum from a healthy cow (Fig. 4C) or a clinically suspected BSE-negative cow (data not shown). On the contrary, obvious immunoreactive spots corresponding to GFAP were observed in the serum from the autoantibody-positive BSE cow (Fig. 4D).

3.4 Positivity of anti-GFAP autoantibody and GFAP in serum

The data from each cow concerning the presence of GFAP and its autoantibody in the serum are shown in Fig. 5. Anti-GFAP autoantibody was determined by dot-blot analysis, as described in Section 2, and GFAP in the serum was analyzed by 2-D immunoblotting shown in Fig. 4. GFAP in the serum was detected in 2 of 15 healthy cattle (13.3%), 6 of 20 clinically suspected BSE-negative cattle (30.0%) and 12 of 18 BSE cattle (66.7%). Compared with the healthy cattle ($p = 0.0063$) or the clinically suspected BSE-negative cattle ($p = 0.0530$), the BSE cattle had GFAP in the serum in a high ratio. On the other hand, an anti-GFAP antibody in the serum was detected in 2 of 15 healthy cattle (13.3%), 4 of 20 clinically suspected BSE-negative cattle (20.0%), and 9 of 18 BSE cattle (50.0%). Similar to GFAP in the serum, the BSE
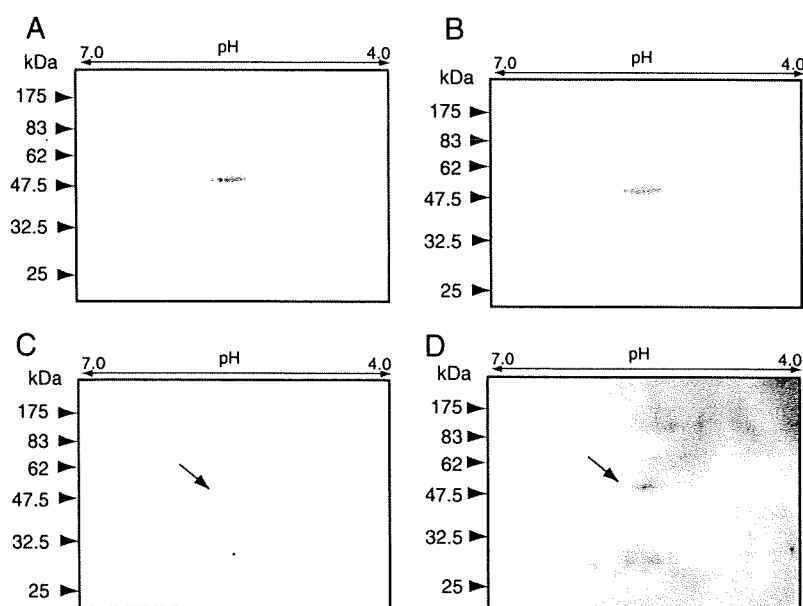
Figure 4. Detection of serum GFAP. Purified bovine GFAP (10 μg) used as a control was subjected to 2-D (p/ 4.0–7.0) PAGE (A, CBB stain) and the protein (1.0 μg) was electroblotted onto a nylon membrane. The blotted protein was confirmed to bind to a polyclonal antibody against human GFAP (B); this antibody has cross-reactivity with bovine GFAP having a 53 kDa molecular weight. Serum (4 μL) proteins from a healthy cow (cow no. 2 in Fig. 4B) (C) or from a BSE cow (cow no. 2 in Fig. 4B) (D) were subjected to 2-D (p/ 4.0–7.0) PAGE and subsequent immunoblotting analysis with the same anti-GFAP antibody as used in (B). Positive signal spots having the same p/ (approximately 5.0–5.5) and molecular weight (50–53 kDa) as shown in (B) were demonstrated in (D) but not in (C).

cattle had the anti-GFAP autoantibody in a high ratio, compared with the healthy cattle ($p = 0.0599$) or the clinically suspected BSE-negative cattle ($p = 0.1087$). Furthermore, the positive ratios of both the autoantibody and GFAP were 0% in the healthy cattle, 5.0% in the clinically suspected BSE-negative cattle and 44.0% in the BSE cattle (Fig. 5), indicating that the BSE cattle showed a significant relationship between the presence of GFAP and the expression of its autoantibody in the serum when compared with the healthy cattle ($p = 0.0032$) or the clinically suspected BSE-negative cattle ($p = 0.0057$).

4 Discussion

Autoantibody against GFAP was found in the sera of cattle with BSE. Previous studies have reported that GFAP is an intermediate filament protein and that it is the major cytoskeletal component of astrocytes, so it is used as a marker for these cells [11]. Many researchers have reported marked proliferation of astrocytes and increased GFAP expression in the cells in the case of natural scrapie in sheep [12] and in mice infected experimentally with scrapie [1, 13–15]. Aoki et al. found that the sera of animals experimentally infected with kuru and CJD contained autoantibodies against neurofilament proteins [16]. The prevalence of serum that possesses immunoreactivity against neurofilament proteins in prion diseases was 12.7% in kuru and 4–14.5% in CJD. Furthermore, the prevalence in the sera of sheep naturally infected with scrapie was 35% (7/20 sheep) [16]. These studies used ELISA to detect the autoantibodies; however, this method cannot exclude cross-reactivity of the antibodies with other proteins. We have

found clear evidence of autoantibodies against another brain-derived protein, GFAP, by 2-D PAGE following immunoblotting analysis and the antigen was identified using MALDI-TOF-MS. Tiwana et al. [6] showed the presence of autoantibodies against neurofilaments and myelin in sera from cattle with BSE, and they found several similarities between the sequences of the brain-derived proteins and the proteins from *Acinetobacter calcoaceticus*. These authors suggested that the autoantibodies were originally raised against the bacterial molecules in infected cattle that were also suffering from BSE. Sera of BSE-suspected cattle or BSE cattle are sampled after slaughter. In such cases, the blood samples might be contaminated with brain-derived proteins through the practice of stunning and pithing during the slaughter of cattle. However, autoantibodies against brain-derived proteins cannot be expressed in such cases.

Autoantibodies against neuronal proteins were detected in scrapie mouse [17]. Infectious particles causing scrapie might be containing GFAP because the scrapie prion protein (PrP^{sc}) is able to bind to GFAP [18]. In natural infection, autoantibodies against GFAP might be produced by accumulation of PrP^{sc}, which appears to be a component of the infectious particle, bound GFAP [18]. Scrapie agent induces expression of at least one mRNA in the brain neurons [19]. Elevation of GFAP expression was observed in CJD brain, and the increases occurred with no detectable spongiform changes at any time during the disease, suggesting that these GFAP increases cannot be simply a response to neuronal damages [18, 20]. Levels of neuron-specific enolase, GFAP, and neurofilament protein light chains are increased in the cerebrospinal fluid in various diseases and can be interpreted as early signs of brain
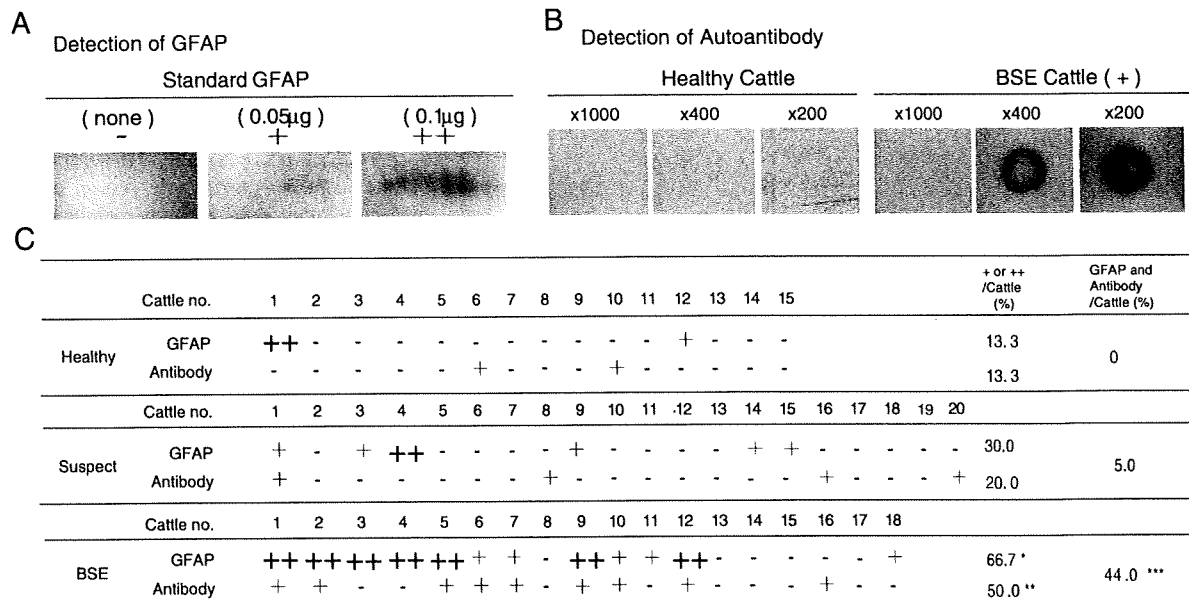
A Detection of GFAP

Standard GFAP

(none) −	(0.05μg) +	(0.1μg) ++

B Detection of Autoantibody

Healthy Cattle			BSE Cattle (+)		
x1000	x400	x200	x1000	x400	x200

C

	Cattle no.	1	2	3	4	5	6	7	8	9	10	11	12	13	14	15	+ or ++ /Cattle (%)	GFAP and Antibody /Cattle (%)
Healthy	GFAP	++	-	-	-	-	-	-	-	-	-	-	+	-	-	-	13.3	0
	Antibody	-	-	-	-	-	+	-	-	-	+	-	-	-	-	-	13.3	

	Cattle no.	1	2	3	4	5	6	7	8	9	10	11	12	13	14	15	16	17	18	19	20		
Suspect	GFAP	+	-	+	++	-	-	-	-	-	+	-	-	-	-	+	+	-	-	-	-	30.0	5.0
	Antibody	+	-	-	-	-	-	-	-	+	-	-	-	-	-	-	-	+	-	-	-	+	20.0	

	Cattle no.	1	2	3	4	5	6	7	8	9	10	11	12	13	14	15	16	17	18		
BSE	GFAP	++	++	++	++	++	+	+	-	++	+	+	++	-	-	-	-	-	+	66.7 *	44.0 ***
	Antibody	+	+	-	-	+	+	+	-	+	+	-	+	-	-	-	+	-	-	50.0 **	

Figure 5. Presence of GFAP and its autoantibody in the sera from cattle. (A) Serum proteins (60 μg) from cattle were separated by 2-D PAGE and then serum GFAP was detected by immunoblotting analysis using the polyclonal antibody as shown in Fig. 3B. The positive signal levels approximately corresponded to more than 0.02 μg (+) and 0.4 μg (++) of standard GFAP (about 4–80 μg/mL in the serum). The results of GFAP levels in healthy, BSE-suspected and BSE cattle are denoted as "−", "+" and "++" (C). (B) Anti-GFAP autoantibody in the serum was detected by dot blotting analysis, using the bovine GFAP standard (0.1 μg), which was reacted with 1000-fold (1000), 400-fold (400) or 200-fold (200) diluted sera from a healthy cow (healthy; no. 2 cattle in (C) or a BSE cow (BSE; no. 2 cattle). Anti-GFAP autoantibody signals are exhibited as "−" and "+", which were determined by using 200-fold diluted serum. No signals as shown in the healthy cattle in (B) are denoted as "−", and positive signals as shown in the BSE cattle in (B) are denoted as "+". Statistical analyses were performed using a nonparametric χ^2 test (Yates' continuity correction) or Fisher's exact method (two-sided). $^*p = 0.0063$ for healthy, $p = 0.0530$ for suspect; $^{**}p = 0.0599$ for healthy, $p = 0.1087$ for suspect; $^{***}p = 0.0063$ for healthy, $p = 0.0113$ for suspect.

damage [21]. The serum concentration of GFAP constitutes a diagnostic biomarker for prognosis in patients with brain disorders such as brain tumors including glioblastomas [22, 23], severe traumatic brain injury [24], and aneurysmal subarachnoid hemorrhage [25]. GFAP was expressed and produced only in the nervous system. This indicates that the astrocytic protein GFAP leaks from the brain into the peripheral blood as a result of localized damage of the blood–brain barrier. However, no detection of anti-GFAP autoantibody was reported in the sera of these diseases. The autoantibody might be produced by the exposure to the antigen during long period of diseases as reported in prion diseases [16]. In fact, astrocytosis is one of the hallmarks of the neuropathology of TSEs, and it is known to appear in accordance with accumulation of the abnormal prion protein in the brain for a long time [1, 15]. In addition, it is reported that the integrity of the blood–brain barrier is harmed in scrapie-infected mice [26, 27]. Taken together with these previous findings, our current findings of the presence of both GFAP and its autoantibody in the sera of BSE cattle in a significantly high incidence suggest that autoantibody production occurred against GFAP that had leaked into the peripheral blood from the brain affected with BSE.

In conclusion, we revealed that either GFAP or its autoantibody was present in the sera of BSE cattle in a significantly high incidence, compared with the incidence in healthy cattle or clinically suspected BSE-negative cattle. In addition, we revealed that there was a significant relationship in BSE cattle between the presence of GFAP and the expression of its autoantibody in the serum. Thus far, there have been no clinical data available for both the BSE cattle and the clinically suspected BSE-negative cattle analyzed in the current study. It remains to be evaluated whether the presence of GFAP or its autoantibody in the serum is related to any aspects of clinical and pathological features. As a surrogate marker for brain diseases including BSE, either GFAP or its autoantibody in the serum might be useful, although diachronic analyses of GFAP and its autoantibody in BSE cattle remain to be performed. In a subsequent investigation, it will be very interesting to discuss about the relationships between the production of autoantibodies against GFAP and aging of cattle for the investigation of the producing process of the autoantibodies and for application to serum diagnosis of BSE.

www.proteomics-journal.com

5 References

[1] Prusiner,S. B., Prions. *Proc. Natl. Acad. Sci. USA* 1998, *95*, 13363–13383.

[2] DeArmond, S. J., Prusiner, S. B., Prion disease. in: Lantos, P. I., Gvaham, D. I., (Eds.), *Greenfield's Neuropathology*, Vol. 2, 6th Edn, Edward Arnold, London 1997, pp. 235–280.

[3] Bruce, M. E., Will, R. G., Ironside, J. W., McConnell, I. *et al.*, Transmissions to mice indicate that new variant CJD is caused by the BSE agent. *Nature* 1997, *389*, 498–501.

[4] Toh, B. H., Gibbs, C. J., Jr., Gajdusek, D. C., Goudsmit, J., Dahl, D., The 200- and 150-kDa neurofilament proteins react with IgG autoantibodies from patients with kuru, Creutz-feldt–Jakob disease, and other neurologic disease. *Proc. Natl. Acad. Sci. USA* 1985, *82*, 3485–3489.

[5] Toh, B. H., Gibbs,C. J., Jr., Gajdusek, D. C., David, D. T., Dahl, D., The 200- and 150-kDa neurofilament proteins react with IgG autoantibodies from chimpanzees ith kuru or Creutzfeldt–Jakob disease; a 62 kDa neurofilament-associated protein reacts with sera from sheep with natural scrapie. *Proc. Natl. Acad. Sci. USA* 1985, *82*, 3894–3896.

[6] Tiwana, H., Wilson, C., Pirt, J., Cartmell, W., Ebringer, A., Autoantibodies to brain components and antibodies to *Acinetobacter calcoaceticus* are present in bovine spongi-form encephalopathy. *Infect. Immun.* 1999, *67*, 6591–6595.

[7] Wilson, C., Hughes, L. E., Rashid, T., Ebringer, A., Bansal, S., Antibodies to acinetobacter bacteria and bovine brain peptides, measured in bovine spongiform encephalopathy (BSE) in an attempt to develop an ante-mortem test. *J. Clin. Lab. Immunol.* 2003, *52*, 023–040.

[8] Laemmli, U. K., Cleavage of structural proteins during the assembly of the head of bacteriophage T4. *Nature* 1970, *227*, 680–685.

[9] Towbin, H., Staehelin, T., Gordon, J., Electrophoretic transfer of proteins from polyacrylamide gels to nitrocellu-lose sheets: procedure and some applications. *Proc. Natl. Acad. Sci. USA* 1979, *76*, 4350–4354.

[10] Dahl, D., Crosby, C. J., Gardner, E. E., Bignami, A., Purifi-cation of the glial fibrillary acidic protein by anion-exchange chromatography. *Anal. Biochem.* 1982, *126*, 165–169.

[11] Malloch, G. D. A., Clark, J. B., Burnet, F. R., Glial fibrillary acidic protein in the cytoskeletal and soluble protein fraction of the developing rat brain. *J. Neurochem.* 1987, *48*, 299–306.

[12] Georgsson, G., Gisladottir, E., Arnadottir, S., Quantitative assessment of the astrocytic response in natural scrapie of sheep. *J. Comp. Pathol.* 1993, *108*, 229–240.

[13] Dormont, D., Delpech, B., Delpech, A., Courcel, M. N. *et al.*, Court, Hyperproduction of glial fibrillary acidic protein (GFA) during development of experimental scrapie in mice. *C R Seances Acad. Sci.* 1981, *293*, 53–56.

[14] Manuelidis, L., Tesin, D. M., Sklaviadis, T., Manuelidis, E. E., Astrocyte gene expression in Creutzfeldt–Jakob disease. *Proc. Natl. Acad. Sci. USA* 1987, *84*, 5937–5941.

[15] DeArmond, S. J., Gonzales, M., Mobley, W. C., Kon, A. A. *et al.*, PrPsc in scrapie-infected hamster brain is spatially and temporally related to histopathology and infectivity titer. *Prog. Clin. Biol. Res.* 1989, *317*, 601–618.

[16] Aoki,T., Gibbs,C. J., Jr., Sotelo, J., Gajdusek,D. C., Hetero-geneic autoantibody against neurofilament protein in the sera of animals with experimental Kuru and Creutzfeldt–Jakob disease and natural scrapie infection. *Infect. Immun.* 1982, *38*, 316–324.

[17] Büeler, H., Aguzzi, A., Sailer, A., Greiner, R. A. *et al.*, Mice devoid of PrP are resistant to scrapie. *Cell* 1993, *73*, 1339–1347.

[18] Oesch, B., Teplow, D. B., Stahl, N., Serban, D. *et al.*, Iden-tification of cellular proteins binding to the scrapie prion protein. *Biochemistry* 1990, *29*, 5848–5855.

[19] Wietgrefe, S., Zupancic, M., Haase, A., Chesebro, B. *et al.*, Cloning of a gene whose expression is increased in scrapie and in senile plaques in human brain. *Science* 1985, *230*, 1177–1179.

[20] Manuelidis, L., Tesin, D. M., Sklaviadis, T., Manuelidis, E. E., Astrocyte gene expression in Creutzfeldt–Jakob disease. *Proc. Natl. Acad. Sci. USA* 1987, *84*, 5937–5941.

[21] Osterlundh, G., Kjellmer, I., Lannering, B., Rosengren, L. *et al.*, Neurochemical markers of brain damage in cere-brospinal fluid during induction treatment of acute lymphoblastic leukemia in children. *Pediatr. Blood Cancer* 2008, *50*, 793–798.

[22] Jung, C. S., Foerch, C., Schänzer, A., Heck, A. *et al.*, Serum GFAP is a diagnostic marker for glioblastoma multiforme. *Brain* 2007, *130*, 3336–3341.

[23] Brommeland, T., Rosengren, L., Fridlund, S., Hennig, R., Isaksen, V., Serum levels of glial fibrillary acidic protein correlate to tumour volume of high-grade gliomas. *Acta Neurol. Scand.* 2007, *116*, 380–384.

[24] Nylén, K., Ost, M., Csajbok, L. Z., Nilsson, I. *et al.*, Increased serum-GFAP in patients with severe traumatic brain injury is related to outcome. *J. Neurol. Sci.* 2008, *240*, 85–91.

[25] Nylén, K., Csajbok, L. Z., Ost, M., Rashid, A. *et al.*, Serum glial fibrillary acidic protein is related to focal brain injury and outcome after aneurysmal subarachnoid hemorrhage. *Stroke* 2007, *38*, 1489–1494.

[26] Wisniewski, H. M., Lossinsky, A. S., Moretz, R. C., Vorbrodt, A. W. *et al.*, Increased blood–brain barrier permeability in scrapie-infected mice. *J Neuropathol. Exp. Neurol.* 1983, *42*, 615–626.

[27] Vorbrodt, A. W., Dobrogowska, D. H., Tarnawski, M., Meeker, H. C., Carp, R. I., Immunocytochemical evaluation of blood-brain barrier to endogenous albumin in scrapie-infected mice. *Acta Neuropathol.* 1997, *93*, 341–348.

Amyloidophilic Compounds for Prion Diseases

Kenta Teruya,[1] Keiichi Kawagoe,[2] Tomohiro Kimura,[1] Chun-jen Chen,[2] Yuji Sakasegawa[1] and Katsumi Doh-ura[1]*

[1]*Department of Prion Research, Tohoku University Graduate School of Medicine, Sendai, Japan, and [2]Tokyo R & D Center, Daiichi Pharmaceutical Co., Ltd., Tokyo, Japan*

Abstract: Recent outbreaks of variant Creutzfeldt-Jakob disease and iatrogenic Creutzfeldt-Jakob disease have aroused great concern in many countries and have necessitated the development of suitable therapies. We have demonstrated that sulfated glycans such as pentosan polysulfate and fucoidan, and amyloidophilic compounds such as amyloid dye derivatives, styrylbenzoazole derivatives, and phenylhydrazine derivatives have efficacies in prion-infected animals. Amyloidophilic compounds present potentialities not only as therapeutic candidates but also as prion amyloid imaging probes for use in nuclear medicine technology such as positron emission tomography. A representative of styrylbenzoazole compounds has been used recently for clinical trials of brain prion amyloid imaging in patients. On the other hand, a representative of phenylhydrazine compounds, compB, displays excellent effectiveness in prolonging the incubation times of infected animals when given orally. However, both its anti-prion effectiveness *in vitro* and its therapeutic efficacy *in vivo* are consistently dependent on the prion strain. This prion-strain-dependency is similarly observed in other amyloidophilic compounds. Therefore, aside from further improvement of the safety profiles and pharmacokinetic properties of such compounds, elucidation and management in the mechanism of the prion strain-dependent effectiveness is necessary. Nevertheless, because compB studies suggest that amyloidophilic compounds are also therapeutic candidates for Alzheimer's disease, amyloidophilic compounds might be attractive as drug candidates for various conformational diseases and hasten development of therapeutic drugs for prion diseases.

Keywords: Sulfated glycan, amyloidophilic chemical, therapy, amyloid imaging, prion disease, Alzheimer's disease.

INTRODUCTION

Transmissible spongiform encephalopathies or prion diseases are a group of fatal neurodegenerative disorders. They include Creutzfeldt-Jakob disease (CJD) and Gerstmann-Sträussler-Scheinker syndrome (GSS) in humans, and scrapie, bovine spongiform encephalopathy, and chronic wasting disease in animals. These disorders are characterized by accumulation of an abnormally folded prion protein (PrPsc) in the central nervous system and the lymphoreticular system. This PrPsc is suggested to be the main component of prion or the prion itself and to be responsible for pathogenesis [1]. It is formed from the normal isoform of PrP (PrPc) and contains more β-sheet composition in the secondary structure [2]; its accumulation is characterized by amyloid fibrils [3].

The mechanism of PrPsc formation from PrPc remains controversial, but both the heterodimer formation [4] and seed-dependent polymerization [5] might be involved. Especially, enrollment of the seed-dependent polymerization is well supported by PrPsc amplification *in vitro* using the protein misfolding cyclic amplification method [6]. This mechanism is inferred also for formation of misfolded protein deposits observed in other conformational diseases such as amyloidoses, Alzheimer's disease, Parkinson's disease, and Huntington's disease [7]. These misfolded protein deposits are well characterized as disease hallmarks detected by histochemical techniques and immunohistochemical techniques. Amyloid staining with amyloidophilic chemicals such as Congo red and thioflavin S is a histochemical technique to detect those misfolded protein deposits in the tissues [8-10].

Recent outbreaks of acquired forms of prion diseases, such as variant CJD [11] through consumption of bovine-prion-contaminated foods and iatrogenic CJD [12] through use of cadaveric growth hormone or dura grafts, have necessitated the development of prophylactic and therapeutic interventions. Regarding the situation in Japan, 1072 cases of prion diseases were reported from April 1999 to February 2008; 75 of those cases (7.0%) had acquired prion diseases including one variant CJD and 74 dural iatrogenic CJD. Since the first case appeared in 1991, 132 cases of dural iatrogenic CJD have been recognized; many people remain at high-risk for dural iatrogenic CJD.

Pioneering studies for exploring therapeutic candidates using persistently prion-infected cells were done by Caughey and his colleagues [13,14]. They showed that Congo red and sulfated glycans inhibit PrPsc formation in prion-infected neuroblastoma cells. Following this discovery, Ingrosso and his colleagues [15] showed the potency of Congo red in prion-infected mice. Since the discovery of the therapeutic activity of Congo red, amyloidophilic chemicals such as amyloid dye derivatives and glucosaminoglycan mimetics have been recognized as one class of possible therapeutic candidates for prion diseases [16,17]. Herein, based on our findings, we review the usefulness and limitations of these chemicals as therapeutic candidates.

SULFATED GLYCANS AS GLYCOSAMINOGLYCAN MIMETICS

The PrPc is characterized as a glycosylphosphatidylinositol-anchored cell-surface membrane protein [18]. Results

*Address correspondence to this author at the Department of Prion Research, Tohoku University Graduate School of Medicine, 2-1 Seiryo-cho, Aoba-ku, Sendai 980-8575, Japan; Tel: (+81)-22-717-8232; Fax: (+81)-22-717-7656; E-mail: doh-ura@mail.tains.tohoku.ac.jp

of earlier studies have suggested that PrPc binds to polyanionic compounds such as heparin, a highly sulfated glycosaminoglycan [14]. Along with this observation, immunohistochemical staining of the brain tissues from prion-infected hamsters and a patient with GSS revealed co-localization of sulfated glycosaminoglycans with abnormal PrP deposition presumably composed of PrPsc [19]. Thus, sulfated glycosaminoglycan mimetics such as sulfated glycans have been proposed to be drug candidates to inhibit the interaction between PrPc and PrPsc [13,14]. The first attempt to treat prion-infected animals with sulfated glycans such as dextran sulfate (Fig. 1a) and pentosan polysulfate (PPS) (Fig. 1b) was performed by Diringer and Ehlers [20]. The effectiveness of these sulfated glycans *in vivo*, however, was restricted to administration either before or soon after peripheral infection. Sulfated glycans injected intraperitoneally inhibit prion replication in the lymphoreticular system, which is involved in the delivery of prion from the gut to the brain [21,22]. Therefore, treatment with sulfated glycans was thought to be preventive only for those individuals with accidental inoculation in the periphery [23].

Fucoidan (Fig. 1c), a complex sulfated fucosylated poly-saccharide, is a type of sulfated glycan that is abundantly present in foods that are consumed daily in Japan, such as seaweed. We previously reported delays of the disease onset in enterally prion-infected mice by oral ingestion of dietary seaweed fucoidan when given for 6 days after the infection, but not when given before the infection [24]. This effect reaches the maximum level at a concentration of 2.5% or less of fucoidan in feed. This effectiveness might result from some proportions of fucoidan that are absorbed from the gut into the blood [25], although little more is known of the detailed pharmacology of ingested fucoidan.

The sulfated glycans described above are such hydrophilic macromolecules that they penetrate only slightly into the brain, which is the main target organ of prion diseases. The blood-brain barrier (BBB) is an issue of utmost concern in the treatment of prion diseases because chemicals with large molecules or large electric charges have difficulty penetrating into the brain [26]. Aside from the BBB, the brain has barriers of two other types: the blood-cerebrospinal fluid barrier and the cerebrospinal fluid-brain barrier. Among them, the cerebrospinal fluid-brain barrier is the loosest: chemicals encountering difficulty in penetrating through the BBB can be expected to enter the brain parenchyma when injected into the cerebrospinal fluid spaces such as the cerebral ventricules.

That idea was verified through animal experiments [27] in which prion-infected mice treated with continuous PPS infusion into the cerebral ventricule survive remarkably longer than the non-treated prion-infected mice. Cerebro-ventricularly infused PPS suppresses abnormal PrP deposition as well as neurodegenerative changes and infectivity in the brain hemisphere of injection. On the opposite brain hemisphere, however, these are not well suppressed. The findings indicate the limitation of cerebroventricular administration treatment using large, strongly charged molecules. Cerebroventricular drug administration is an alternative treatment method to obviate the BBB hurdle, but drug diffusion into the brain parenchyma remains vital for successful treatment.

Based on the animal experiments described above, a clinical approach with long-term cerebroventricular PPS administration has been carried out in more than 25 patients with various prion diseases [28]. Although its therapeutic efficacy remains to be confirmed, preliminary clinical experience indicates prolonged survival in several patients receiving long-term PPS [28-30]. Further prospective investigation of PPS administration is necessary to obtain high-quality evidence for its clinical benefits. However, this treatment has weaknesses, one of which has already been discussed. Another is the requirement for surgical implantation of a continuous infusion pump and a cerebroventricular catheter, which might come to obstruct extension of clinical trials because of the risks of prion contamination that are attendant with operating rooms and operation instruments.

AMYLOID DYE DERIVATIVES AND OTHER AMYLOIDOPHILIC CHEMICALS

As described earlier, Congo red (Fig. 1d) inhibits new formation of PrPsc in prion-infected cells and prolongs the incubation period of infected animals when administered prophylactically. Congo red binds to either PrPc or PrPsc and blocks the formation of PrPsc from PrPc [14,31]. However, Congo red can not be used as a therapeutic drug because of both its inability to cross the BBB and because of its teratogenic and carcinogenic properties. Since the discovery of Congo red, several structure-activity relationship studies of amyloid dye chemicals have been performed, but no promising candidates showing effectiveness *in vivo* were reported.

Recently, the most advanced progress with amyloidophilic compounds that readily permeate the BBB has been made in the field of diagnosis of Alzheimer's disease (AD) [32,33]. Many amyloidophilic chemicals have been developed as imaging probes to visualize amyloid deposits in the brains of AD patients using nuclear medicine technology such as positron emission tomography (PET) and single-photon emission computed tomography [34,35]. Some of these chemicals are also useful to portray abnormal PrP amyloid deposits in brain tissues affected by some prion diseases [36-38], which indicates that such amyloidophilic compounds are not disease-specific. Nevertheless, these chemicals are useful to evaluate amyloid deposits because anatomical distributions of pathological deposition differ among diseases. For example, Aβ plaques of AD are seldom observed in the cerebellum, although PrP amyloid plaques of GSS or variant CJD are abundantly observed there.

Fig. (2) presents a diagram of hypothetical mechanism of therapeutic amyloidophilic chemicals. In a brain affected with prion disease or AD, it is suggested that normal protein molecules bind to abnormal protein seeds. They are subsequently converted into abnormal protein aggregates [5]. Thereafter, abnormal protein aggregates cause cell damage by unknown mechanisms. In the presence of amyloidophilic chemicals, they bind to normal protein molecules and abnormal protein seeds and stabilize them. Then, abnormal protein aggregates are not produced, and no cell damage is
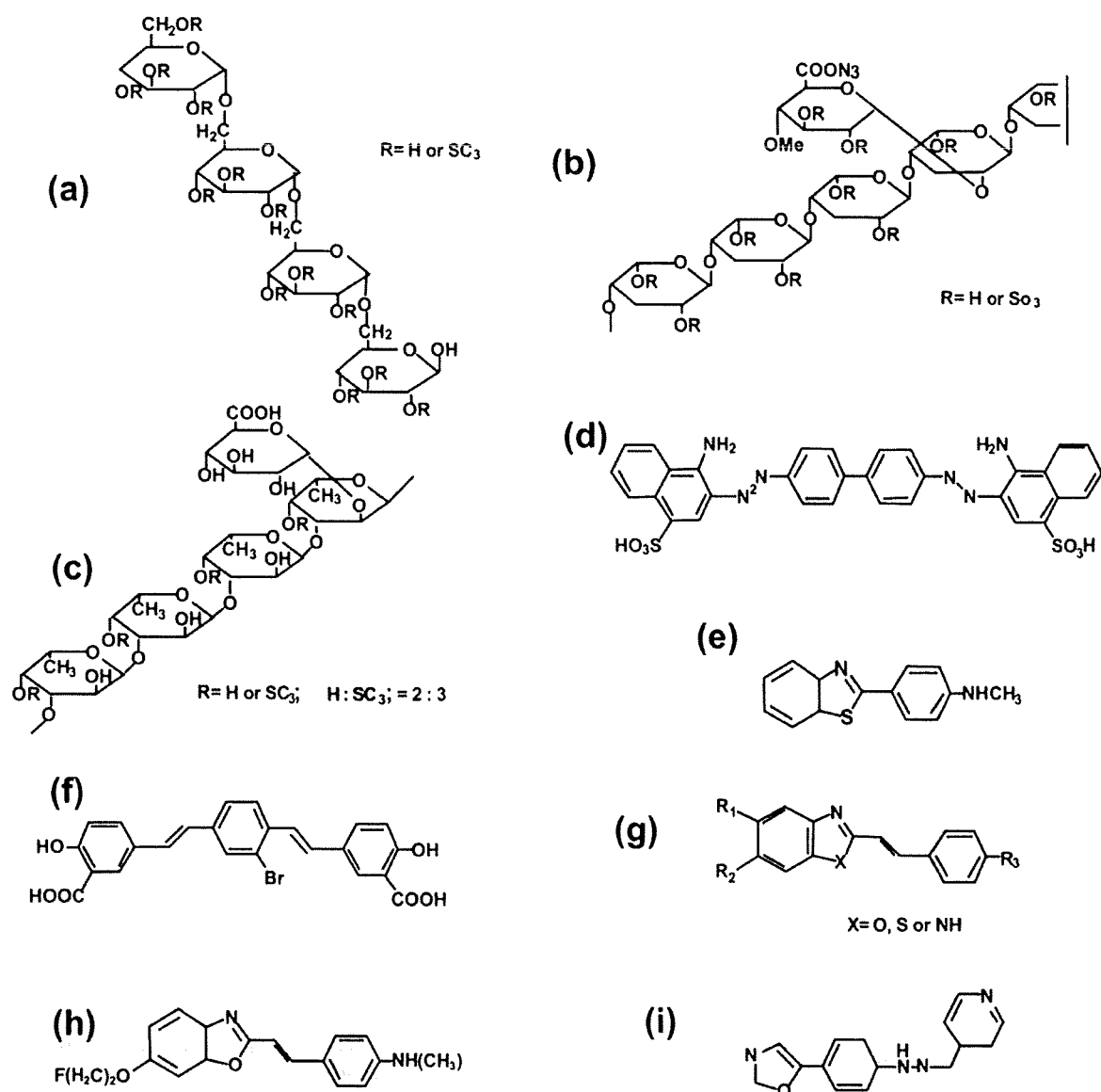
Fig. (1). Amyloidophilic compounds with therapeutic activities:
(a) dextran sulfate, (b) pentosan polysulfate, (c) fucoidan, (d) Congo red, (e) BTA-1, (f) BSB, (g) styrylbenzoazole, (h) BF-168, and (i) compB.

caused. This context is also suggested in other conformational diseases [7]. Consequently, amyloidophilic chemicals might be applicable for therapy of the diseases.

BTA-1 AND BSB

To evaluate the applicability of recently developed amyloidophilic chemicals to therapeutic candidates for prion diseases, two candidate compounds were first examined: a thioflavin derivative, 2-[4'-(methylamino)phenyl] benzothiazole (BTA-1) [39] (Fig. 1e) and a Congo red derivative, (*trans*, *trans*),-1-bromo- 2,5-bis-(3-hydroxycarbonyl-4-hydroxy)styrylbenzene (BSB) [40] (Fig. 1f). Visualization of abnormal PrP deposition in the brain using BTA-1 or BSB was demonstrated using histopathological specimens from prion disease patients. Both chemicals fluorescently labeled

most of the compact PrP plaques in the cerebellar cortices of GSS patients [41]. In another experiment [42], BSB reactivity was observed with amyloid deposits in various amyloidotic conditions such as familial amyloidotic polyneuropathy, AA and AL amyloidosis, and dialysis-related amyloidosis.

Both compounds are potent in inhibiting PrPsc formation in neuroblastoma cells infected with the RML prion [41,43] (EC_{50}; 4 nM for BTA-1 and 1.4 μM for BSB). However, neither chemical is effective in cells infected with the Fukuoka-1 prion or the 22L prion [41,44]. Treatment with an intravenous injection of BSB at 40 mg/kg body weight at day 45 and day 60 post-infection prolongs the incubation period of Tga20 mice [45] cerebrally infected with the RML prion
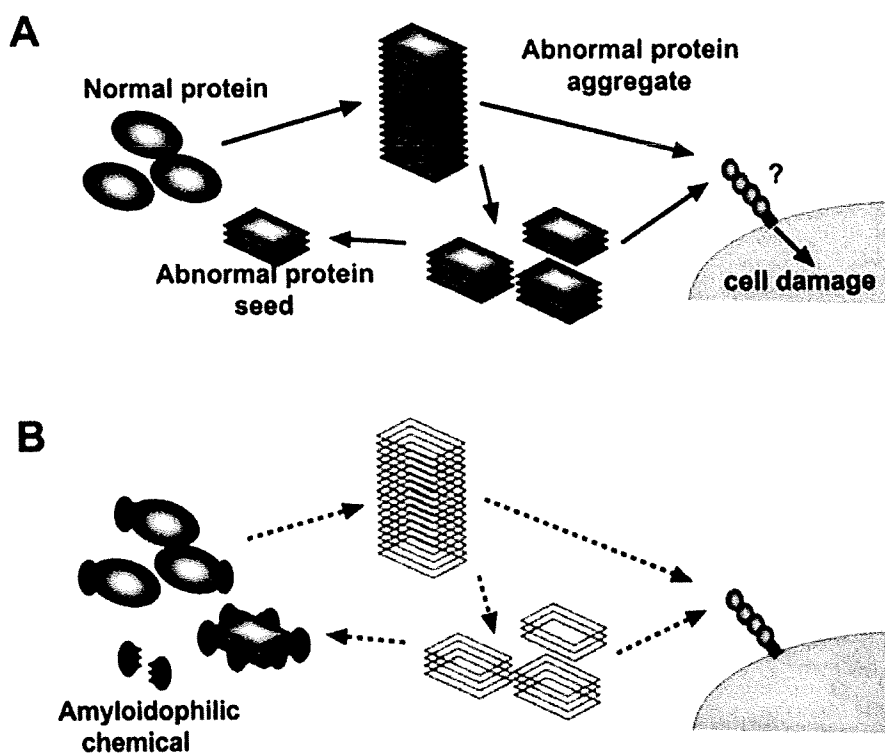
Fig. (2). Hypothetical mechanism of therapeutic amyloidophilic compounds.

A. Normal protein molecules bind to abnormal protein seeds. Then they are converted into abnormal protein aggregates. Thereafter, abnormal protein aggregates cause cell damage by unknown mechanisms.

B. In the presence of amyloidophilic compounds, they bind to normal protein molecules and abnormal protein seeds and stabilize them. Consequently, abnormal protein aggregates are not produced; no cell damage is caused.

by 13.6% (77.6 days in the BSB-treated group vs. 68.3 days in the vehicle control), although no significant prolongation is obtained from an identical treatment for Tg7 mice [46] infected with the 263K prion. Actually, BSB is less toxic than Congo red and is effective in prolonging the incubation period of the RML-infected Tga20 mice despite being introduced at a late stage of the infection. These characteristics suggest that these chemicals are candidates not only for use as imaging probes but also as therapeutic drugs for some prion diseases. Nevertheless, the chemicals have poor permeability into the brain.

STYRYLBENZOAZOLE DERIVATIVES

Most styrylbenzoazole derivatives (Fig. **1g**) that have been tested display better permeability into the brain [47]. Some of them clearly label abnormal PrP aggregates in the brain specimens from human prion diseases. Most such chemicals inhibit abnormal PrP formation in RML prion-infected cells with EC_{50} values in the nanomolar range, indicating that they represent the most potent classes of inhibitor ever reported. Treatment with an intravenous injection of a representative chemical, 2-(5-(2-fluoroethoxy)benzo[d]oxazol-2-yl)vinyl)-*N*-methylbenzenamine (BF-168) (Fig. **1h**), at 4 mg/kg body weight at days 28, 35, 42, and 49 post-infection prolongs the lives of mice that have been infected cerebrally with the RML prion by 8.4% (72.2 days in the BF-168-treated group vs. 66.6 days in the vehicle control). However, BF-168 shows pathogen-dependent

efficacy and no effects in mice infected with the 263K prion, similar to BSB.

Actually, BF-168 is excellent in wash-out from the brain as well as in permeability into the brain. Therefore, limited efficacy of BF-168 in prolonging the lives of prion-infected mice might be attributable to its prompt wash-out property. As might be expected, these properties of BF-168 are suitable for imaging probes rather than for therapeutic chemicals. In fact, one intravenous injection of BF-168 at 0.5 mg/kg body weight, which is a 20 times smaller dose than BSB used for *in vivo* PrP amyloid imaging, is sufficient to penetrate into the brain and bind to abnormal PrP aggregates *in vivo*. Clear PrP amyloid imaging by BF-168 is obtained one hour (at most) after injection, although 24 h is necessary for BSB to wash-out non-binding molecules from the brain.

Based on these findings, a clinical trial of brain PET imaging with BF-227, a BF-168 derivative, has been carried out in patients with prion diseases of various types. Although its diagnostic usefulness remains to be confirmed, preliminary experience indicates elevated uptake of the chemical in the brain of the patients with some prion diseases, such as GSS.

PHENYLHYDRAZINE DERIVATIVES

The efficacies of the chemicals described above are not remarkable. In fact, they are rather limited, possibly because of the insufficiency of their persistence in the brain at

sufficiently high concentrations to block PrPsc formation. Daily oral intake rather than several intravenous shots of a chemical are much easier and more suitable for maintaining elevated brain chemical levels, as long as the chemical is readily taken up into the brain when orally administered. Phenylhydrazine derivatives are potentially such orally available chemicals that have been newly developed (Table 1). One of them, 1-(4-(oxazol-5-yl)phenyl)-2-((pyridin-4-yl)methylene)hydrazine (compB) (Fig. 1i), has been thoroughly tested for both its antiprion activity *in vitro* and its therapeutic efficacy *in vivo* [48].

This compound inhibits PrPsc formation in prion-infected neuroblastoma cells in a prion-strain-dependent manner similarly to amyloidophilic chemicals described above: effectively for RML prion and marginally for 22L prion and Fukuoka-1 prion. It extends the incubation period to 2.3 times that of the control when the highest dose (300 mg/kg/day) is given orally to cerebrally RML prion-infected mice from inoculation until the terminal stage of disease (Fig. 3). The compound exerts therapeutic efficacy in a prion strain-dependent manner such as that observed in the cell

culture study: most effective for RML prion, less effective for 22L prion or Fukuoka-1 prion, and marginally effective for 263K prion. Its effectiveness depends on an early start of administration. The glycoform pattern of PrPsc in treated mice is modified and shows predominance of the diglycosylated form resembling that of 263K prion, suggesting that diglycosylated forms of PrPsc might be least sensitive or resistant to the compound.

Phenylhydrazine derivatives described here were originally designed as lead chemicals for either the amyloid imaging probes or the therapeutic drugs of AD [49]. In fact, radio-labeled compB administered intravenously easily penetrates into the brain and binds to $A\beta$ deposits (senile plaques) in the brain of AD model mice modified from Tg2576 [50] (Fig. 4). In addition, compB and other phenylhydrazine chemicals are very effective *in vitro* in inhibiting either $A\beta$ amyloid formation or $A\beta$ amyloid-heparin binding [49,51] (Table 1). Moreover, preliminary studies have demonstrated that compB has inhibitory efficacy for $A\beta$ deposition in AD model mice [51].

CompB is lipophilic and has an excellent permeability

RML prion infection in Tga20 mice — 300 mg/kg/day, 225 mg/kg/day, 150 mg/kg/day, control — Days from infection to death (50, 100, 150, 200)

22L prion infection in Tga20 mice — 300 mg/kg/day, control — Days from infection to death (50, 70, 90, 110, 130, 150)

Fukuoka-1 prion infection in Tga20 mice — 300 mg/kg/day, control — Days from infection to death (50, 70, 90, 110, 130, 150, 170)

263K prion infection in Tg7 mice — 300 mg/kg/day, control — Days from infection to death (40, 50, 60, 70, 80, 90, 100)

263K prion infection in Syrian hamsters — 300 mg/kg/day, control — Days from infection to death (90, 110, 130, 150, 170)
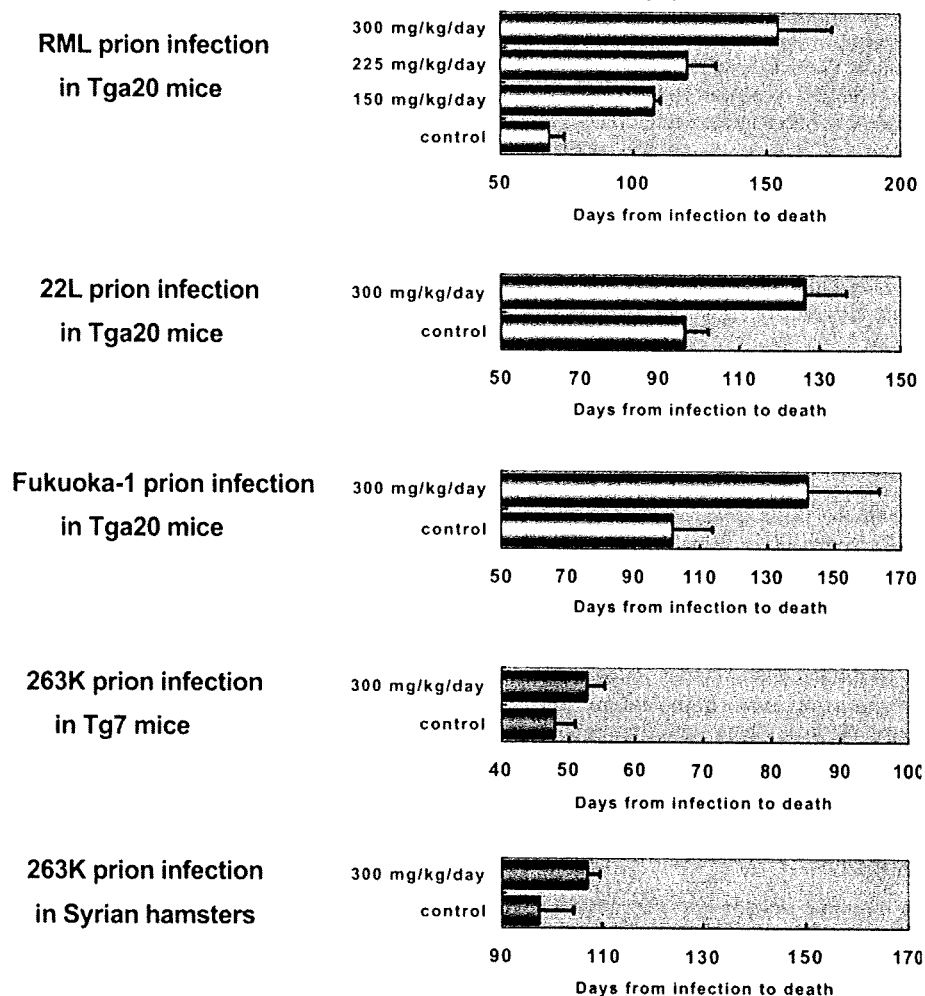
Fig. (3). Therapeutic effects of compB in prion disease mouse models.
Treatment with oral compB administration commences immediately after the cerebral infection and continues to the terminal stage of disease.
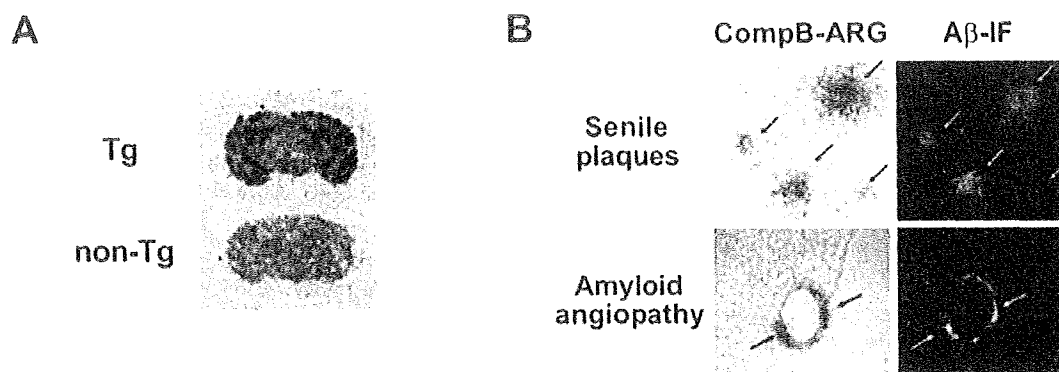
A   **B**   CompB-ARG   Aβ-IF

Tg

non-Tg

Senile
plaques

Amyloid
angiopathy

Fig. (4). Amyloid imaging of compB in an Alzheimer's disease mouse model.

A. Autoradiogram of the brain tissue section from an Alzheimer's disease model mouse (Tg) or a control mouse (non-Tg) with an intravenous injection of radio-labeled compB. The brains were obtained 5 h after injection.

B. Microautoradiogram (CompB-ARG) and Aβ immunohistochemistry (Aβ-IF) of an identical section from the same brain tissue of an Alzheimer's disease model mouse shown in **A**.

into the brain involving no active efflux system [48,51]. However, aside from its low metabolic stability in mouse liver microsome, it has high inhibition activities against several common P450 isozymes, which potentially causes a drug-drug interaction problem [51]. Therefore, the safety properties and pharmacokinetic parameters of this compound must be improved before its clinical application can be considered.

FURTHER IMPROVEMENT

The findings of amyloidophilic compounds described here indicate that the compounds are useful not only for prion amyloid imaging but also for therapy. Especially, the findings related to an orally available amyloidophilic chemical, compB, are encouraging. However, disease progression is not halted even when treatment commences immediately after the infection and continues to the terminal stage of disease.

One reason for this limited effectiveness might be connected with the prion strain-dependent efficacies of the amyloidophilic compounds. Prion strains definitely influence the outcomes of treatment with the compounds. The compounds are most effective against RML prion but less effective against 22L prion and Fukuoka-1 prion either *in vitro* or *in vivo*. They are never effective or only marginally effective against the 263K prion. Interestingly, the PrPsc glycoform patterns observed in the compB-treated mice are predominantly diglycosylated and similar to that of 263K prion, although a monoglycoform predominant pattern is observed in non-treated mice [48]. Such pattern characteristics suggest that limitations of compB efficacy might result from the appearance of compB-resistant diglycoform predominant prions.

Another possible reason for the limited effectiveness might be related to pharmacokinetic properties of the compounds: CompB and BF-168, but not BSB are washed rapidly out from either the brain or the blood. Contrasting BF-168 to BSB shows that BSB prolongs the incubation periods of infected animals significantly longer than BF-168, although BSB requires less frequent intravenous injections
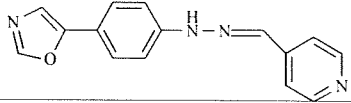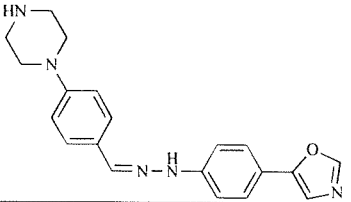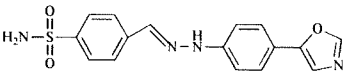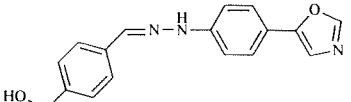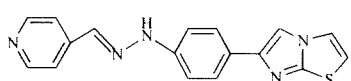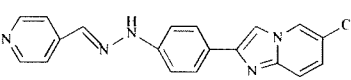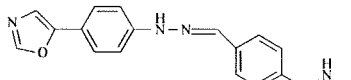
and later application in the disease stage than BF-168. Therefore, not only permeability but also retention of chemicals in the brain is apparently important for better efficacies *in vivo*. In addition, metabolic stability of chemicals is definitely influential on their effectiveness.

Recently, Sigurdson and his colleagues observed prion strain-dependent fluorescence spectral shifts of luminescent conjugated polymers composed of thiophene derivatives when bound to PrPsc, demonstrating prion strain-dependent conformational properties of PrPsc [52], because the fluorescence spectra reflects distributions of the dihedral rotational angles among the monomeric units of the polymers [53,54]. In addition, the correlation between the dihedral rotational angle and the spectra gives insight into the binding mode of Congo red to amyloid [55,56]. On the other hand, rotational freedom between the aromatic rings of Congo red derivatives is important for their antiprion activities [31]. Restriction of the rotational freedom at the center of the compounds reduces the antiprion activities. In fact, compB comprises two aromatic ring parts connected by hydrazone in which free rotation is obtained at the imino nitrogen (-NH-). Similar compounds, 8-hydroxy-8-quino-linylhydrazone-2-quinolinecarboxaldehyde (QCQH in the reference) and 2-quinolinylhydrazone-2-pyridinecar-boxaldehyde (PCQH in the reference) which were tested as quinoline derivatives, also have excellent antiprion activities [57]. These findings indicate that elucidation of the interaction between chemicals and PrPsc at the atomic level is necessary to facilitate further improvement of therapeutic candidates.

CONCLUSION

Amyloidophilic compounds are useful as both prion amyloid imaging probes and therapeutic candidates for prion diseases. The mechanism of the prion strain-dependent effectiveness of these compounds must be elucidated and managed. Nevertheless, the identification of compB, an orally available amyloidophilic chemical, encourages the pursuit of chemotherapy for prion diseases. Drug search and development for prion diseases reportedly does not interest pharmaceutical companies because of the limited number of

Table 1.   In Vitro Activities of Phenylhydrazine Derivatives

Compound	Chemical structure	Molecular weight	Octanol-water distribution coefficient (LogD$_{6.8}$)	Inhibition of PrPsc formation (EC$_{50}$, nM)	Inhibition of Aβ amyloid formation (EC$_{50}$, μM)	Inhibition of Aβ amyloid-heparin binding (EC$_{50}$, μM)
CompB		264	4.1	0.06	2.9	1.1
CompD1		347	2.2	100	8.1	0.9
CompD2		342	3.6	10	2.6	0.4
CompD3		293	3.2	1	1.5	0.9
CompD4		319	Not determined	1	1.1	0.4
CompD5		347	4.7	1	0.2	0.3
CompD6		306	2.4	10	3.1	1.2

patients. However, a therapeutic linkage between prion diseases and other amyloidotic conditions such as AD, demonstrated by compB, might accelerate the development of therapeutic drugs for prion diseases.

ACKNOWLEDGMENTS

ABBREVIATIONS

AD	=	Alzheimer's disease
BBB	=	Blood brain barrier
BF-168	=	2-(5-(2-fluoroethoxy)benzo[d]oxazol-2-yl)vinyl)-N-methylbenzenamine
BSB	=	(trans, trans),-1-bromo- 2,5-bis-(3-hydroxycarbonyl-4-hydroxy)styrylbenzene
BTA-1	=	2-[4'-(methylamino)phenyl] benzothiazole
CJD	=	Creuzfeldt-Jakob disease
compB	=	1-(4-(oxazol-5-yl)phenyl)-2-((pyridin-4-yl)methylene)hydrazine
EC$_{50}$	=	dose producing 50% maximal effect
GAG	=	Glycosaminoglycan
GSS	=	Gerstmann-Sträussler-Scheinker syndrome
PET	=	Positron emission tomography
PPS	=	Pentosan polysulfate
PrPc	=	Normal isoform of prion protein
PrPsc	=	Abnormal isoform of prion protein

REFERENCES

[1]   Prusiner, S.B. *Science*, 1991, *252*, 1515.
[2]   Caughey, B.W.; Dong, A.; Bhat, K.S.; Ernst, D.; Hayes, S.F.; Caughey, W.S. *Biochemistry*, 1991, *30*, 7672.
[3]   Prusiner, S.B.; McKinley, M.P.; Bowman, K.A.; Bolton, D.C.; Bendheim, P.E.; Groth, D.F.; Glenner, G.G. *Cell*, 1983, *35*, 349.
[4]   Cohen, F.E.; Pan, K.M.; Huang, Z.; Baldwin, M.; Fletterick, R.J.; Prusiner, S.B. *Science*, 1994, *264*, 530.
[5]   Come, J.H.; Fraser, P.E.; Lansbury, P.T., Jr. *Proc. Natl. Acad. Sci. USA*, 1993, *90*, 5959.
[6]   Saborio, G.P.; Permanne, B.; Soto, C. *Nature*, 2001, *411*, 810.
[7]   Carrell, R.W.; Lomas, D.A. *Lancet*, 1997, *350*, 134.
[8]   Fred, P.; Anisimov, S.V.; Popovic, N. *Brain Res. Rev.*, 2007, *53*, 135.
[9]   Divry, P. *J. Belg. Neurol. Psychiatry*, 1927, *27*, 643.
[10]   Kelényi, G. *Acta Neuropathol.*, 1967, *7*, 336.
[11]   Will, R.G.; Ironside, J.W.; Zeidler, M.; Cousens, S.N.; Estibeiro, K.; Alperovitch, A.; Poser, S.; Pocchiari, M.; Hofman, A.; Smith, P.G. *Lancet*, 1996, *347*, 921.
[12]   Brown, P.; Brandel, J.P.; Preece, M.; Sato, T. *Neurology*, 2006, *67*, 389.
[13]   Caughey, B.; Raymond, G.J. *J. Virol.*, 1993, *67*, 643.
[14]   Caughey, B.; Brown, K.; Raymond, G.J.; Katzenstein, G.E.; Thresher, W. *J Virol.*, 1994, *68*, 2135.
[15]   Ingrosso, L.; Ladogana, A.; Pocchiari, M. *J. Virol.*, 1995, *69*, 506.
[16]   Cashman, N.R.; Caughey, B. *Nat. Rev. Drug Discov.*, 2004, *3*, 874.
[17]   Trevitt, C.R.; Collinge, J. *Brain*, 2006, *129*, 2241.
[18]   Stahl, N.; Borchelt, D.R.; Hsiao, K.; Prusiner, S.B. *Cell*, 1998, *51*, 229.
[19]   Snow, A.D.; Wight, T.N.; Nochlin, D.; Koike, Y.; Kimata, K.; Dearmond, S.J.; Prusiner, S. *Lab. Invest.*, 1990, *63*, 601.
[20]   Diringer, H.; Ehlers, B. *J. Gen. Virol.*, 1991, *72*, 457.
[21]   Farquhar, C.; Dickinson, A.; Bruce, M. *Lancet*, 1999, *353*, 117.
[22]   Mabbott, N.A.; MacPherson, G.G. *Nat. Rev. Microbiol.*, 2006, *4*, 201.
[23]   Dealler, S. *Lancet*, 1998, *351*, 600.
[24]   Doh-ura, K.; Kuge, T.; Uomoto, M.; Nishizawa, K.; Kawasaki, Y.; Iha, M *Antimicrob. Agents Chemother.*, 2007, *51*, 2274.
[25]   Irhimeh, M.R.; Fitton, J.H.; Lowenthal, R.M.; Kongtawelert, P. *Methods Find. Exp. Clin. Pharmacol.*, 2005, *27*, 705.
[26]   Jong, A.; Huang, S.H. *Curr. Drug Targets Infect. Disord.*, 2005, *5*, 65.
[27]   Doh-ura, K.; Ishikawa, K.; Murakami-Kubo, I.; Sasaki, K.; Mohri, S.; Race, R.; Iwaki, T. *J. Virol.*, 2004, *78*, 4999.
[28]   Rainov, N.G.; Tsuboi, Y.; Krolak-Salmon, P.; Vighetto, A.; Doh-Ura, K. *Expert Opin. Biol. Ther.*, 2007, *7*, 713.
[29]   Parry, A.; Baker, I.; Stacey, R.; Wimalaratna, S. *J. Neurol. Neurosurg. Psychiatry*, 2007, *78*, 733.
[30]   Bone, I.; Belton, L.; Walker, A.S.; Darbyshire, *J. Eur. J. Neurol.*, 2008, *15*, 458.
[31]   Demaimay, R.; Harper, J.; Gordon, H.; Weaver, D.; Chesebro, B.; Caughey, B. *J. Neurochem.*, 1998, *71*, 2534.
[32]   Okamura, N.; Suemoto, T.; Shimadzu, H.; Suzuki, M.; Shiomitsu, T.; Akatsu, H.; Yamamoto, T.; Staufenbiel, M.; Yanai, K.; Arai, H.; Sasaki, H.; Kudo, Y.; Sawada, T. *J. Neurosci.*, 2004, *24*, 2535.
[33]   Okamura, N.; Suemoto, T.; Furumoto, S.; Suzuki, M.; Shimadzu, H.; Akatsu, H.; Yamamoto, T.; Fujiwara, H.; Nemoto, M.; Maruyama, M.; Arai, H.; Yanai, K.; Sawada, T.; Kudo, Y. *J. Neurosci.*, 2005, *25*, 10857.
[34]   Cai, L.; Innis, R.B.; Pike, V.W. *Curr. Med. Chem.*, 2007, *14*, 19.

[35]   Furumoto, S.; Okamura, N.; Iwata, T.; Yanai, K.; Arai, H.; Kudo, Y. *Curr. Top. Med. Chem.*, 2007, *7*, 1773.
[36]   Bresjanac, M.; Smid, L.M.; Vovko, T.D.; Petric, A.; Barrio, J.R.; Popovic, M. *J. Neurosci.*, 2003, *23*, 8029.
[37]   Sadowski, M.; Pankiewicz, J.; Scholtzova, H.; Tsai, J.; Li, Y.; Carp, R.I.; Meeker, H.C.; Gambetti, P.; Debnath, M.; Mathis, C.A.; Shao, L.; Gan, W.B.; Klunk, W.E.; Wisniewski, T. *J. Neuropathol. Exp. Neurol.*, 2004, *63*, 775.
[38]   Smid, L.M.; Vovko, T.D.; Popovic, M.; Petric, A.; Kepe, V.; Barrio, J.R.; Vidmar, G.; Bresjanac. M. *Brain Pathol.*, 2006, *16*, 124.
[39]   Mathis, C.A.; Bacskai, B.J.; Kajdasz, S.T.; McLellan, M.E.; Frosch, M.P.; Hyman, B.T.; Holt, D.P.; Wang, Y.; Huang, G.F.; Debnath, M.L.; Klunk, W.E. *Bioorg. Med. Chem. Lett.*, 2002, *12*, 295.
[40]   Skovronsky, D.M.; Zhang, B.; Kung, M.P.; Kung, H.F.; Trojanowski, J.Q.; Lee, V.M. *Proc. Natl. Acad. Sci. USA*, 2000, *97*, 7609.
[41]   Ishikawa, K.; Doh-ura, K.; Kudo, Y.; Nishida, N.; Murakami-Kubo, I.; Ando, Y.; Sawada, T.; Iwaki, T. *J. Gen. Virol.*, 2004, *85*, 1785.
[42]   Ando, Y.; Haraoka, K.; Terazaki, H.; Tanoue, Y.; Ishikawa, K.; Katsuragi, S.; Nakamura, M.; Sun, X.; Nakagawa, K.; Sasamoto, K.; Takesako, K.; Ishizaki, T.; Sasaki, Y.; Doh-ura, K. *Lab. Invest.*, 2003, *83*, 1751.
[43]   Race, R. E.; Caughey, B.; Graham, K.; Ernst, D.; Chesebro, B. *J. Virol.*, 1988, *62*, 2845.
[44]   Nishida, N.; Harris, D.A.; Vilette, D.; Laude, H.; Frobert, Y.; Grassi, J.; Casanova, D.; Milhavet, O.; Lehmann, S. *J. Virol.*, 2000, *74*, 320.
[45]   Fischer, M.; Rulicke, T.; Raeber, A.; Sailer, A.; Moser, M.; Oesch, B.; Brandner, S.; Aguzzi, A.; Weissmann, C. *EMBO J.*, 1996, *15*, 1255.
[46]   Race, R.E.; Priola, S.A.; Bessen, R.A.; Ernst, D.; Dockter, J.; Rall, G.F.; Mucke, L.; Chesebro, B.; Oldstone, M.B. *Neuron*, 1995, *15*, 1183.
[47]   Ishikawa, K.; Kudo, Y.; Nishida, N.; Suemoto, T.; Sawada, T.; Iwaki, T.; Doh-ura, K. *J. Neurochem.*, 2006, *99*, 19.
[48]   Kawasaki, Y.; Kawagoe, K.; Chen, C.J.; Teruya, K.; Sakasegawa, Y.; Doh-ura, K. *J. Virol.*, 2007, *81*, 12889.
[49]   Kawagoe, K.; Motoki, K.; Odagiri, T.; Suzuki, N.; Chen, C.J.; Mimura, T. *PCT Int. Appl.*, 2004, 236.
[50]   Hsiao, K.; Chapman, P.; Nilsen, S.; Eckman, C.; Harigaya, Y.; Younkin, S.; Yang, F.; Cole, G. *Science*, 1996, *274*, 99.
[51]   Suzuki, N.; Chen, C.J.; Kawagoe, K.; Motoki, K.; Odagiri, T.; Mimura, T. unpublished data.
[52]   Sigurdson, C.J.; Nilsson, K.P.R.; Hornemann, S.; Manco, G.; Polymenidou, M.; Schwarz, P.; Leclerc, M.; Hammarström, P.; Wüthrich, K.; Aguzzi, A. *Nat. Method*, 2007, *4*, 1023.
[53]   Nilsson, K.P.R.; Herland, A.; Hammarstrom, P.; Inganaas, O. *Biochemistry*, 2005, *44*, 3718.
[54]   Nilsson, K.P.; Hammarstrom, P.; Ahlgren, F.; Herland, A.; Schnell, E.A.; Lindgren, M.; Westermark, G.T.; Inganas, O. *ChemBioChem*, 2006, *7*, 1096.
[55]   Elhaddaoui, A.; Merlin, J.C.; Delacourte, A.; Turrell, S. *J. Mol. Struct.*, 1992, *267*, 113.
[56]   Miura, T.; Yamamiya, C.; Sasaki M.; Suzuki K.; Takeuchi, H. *J. Raman Spectrosc.*, 2002, *33*, 530.
[57]   Murakami-Kubo, I.; Doh-ura, K.; Ishikawa, K.; Kawatake, S.; Sasaki, K.; Kira, J.; Ohta, S.; Iwaki, T. *J. Virol.*, 2004, *78*, 1281.

ORIGINAL PAPER

Detachment of Brain Pericytes from the Basal Lamina is Involved in Disruption of the Blood–Brain Barrier Caused by Lipopolysaccharide-Induced Sepsis in Mice

Tsuyoshi Nishioku · Shinya Dohgu · Fuyuko Takata ·
Tomoaki Eto · Naoko Ishikawa · Kota B. Kodama ·
Shinsuke Nakagawa · Atsushi Yamauchi · Yasufumi Kataoka

Abstract The blood–brain barrier (BBB) is highly restrictive of the transport of substances between blood and the central nervous system. Brain pericytes are one of the important cellular constituents of the BBB and are multifunctional, polymorphic cells that lie within the microvessel basal lamina. The present study aimed to evaluate the role of pericytes in the mediation of BBB disruption using a lipopolysaccharide (LPS)-induced model of septic encephalopathy in mice. ICR mice were injected intraperitoneally with LPS or saline and were sacrificed at 1, 3, 6, and 24 h after injection. Sodium fluorescein accumulated with time in the hippocampus after LPS injection; this hyperpermeability was supported by detecting the extravasation of fibrinogen. Microglia were activated and the number of microglia increased with time after LPS injection. LPS-treated mice exhibited a broken basal lamina and pericyte detachment from the basal lamina at 6–24 h after LPS injection. The disorganization in the pericyte and basal lamina unit was well correlated with increased microglial activation and increased cerebrovascular permeability in LPS-treated mice. These findings suggest that pericyte detachment and microglial activation may be involved in the mediation of BBB disruption due to inflammatory responses in the damaged brain.

Keywords Blood–brain barrier · Brain pericytes · Basal lamina · Microglia · Lipopolysaccharide · Inflammation

T. Nishioku · S. Dohgu · F. Takata · T. Eto ·
N. Ishikawa · K. B. Kodama · A. Yamauchi ·
Y. Kataoka (✉)
Department of Pharmaceutical Care and Health Sciences,
Faculty of Pharmaceutical Sciences, Fukuoka University,
8-19-1 Nanakuma, Jonan-ku, Fukuoka 814-0180, Japan
e-mail: ykataoka@fukuoka-u.ac.jp

F. Takata · S. Nakagawa · Y. Kataoka
BBB Laboratory, PharmaCo-Cell Co., Ltd, Nagasaki
852-8523, Japan

S. Nakagawa
Department of Pharmacology 1, Graduate School
of Medicine, Nagasaki University, 1-12-4 Sakamoto,
Nagasaki 852-8523, Japan

Introduction

The blood–brain barrier (BBB) strictly restricts the transport of substances between the peripheral circulation and the central nervous system (CNS). This is mediated by the combined presence of tight junctions and membrane transport systems (Hawkins and Davis 2005; Löscher and Potschka 2005). The BBB is primarily formed by brain microvascular endothelial cells that are sealed closely with tight junctions. These cells, together with pericytes, astrocytes, microglia, neurons, and the extracellular matrix, constitute a "neurovascular unit" that is essential

🖄 Springer